Published in final edited form as:
Nat Med. 2014 April ; 20(4): 385–397. doi:10.1038/nm.3482.

MST1 is a novel regulator of apoptosis in pancreatic beta-cells

Amin Ardestani[1], **Federico Paroni**[#1], **Zahra Azizi**[#1], **Supreet Kaur**[#1], **Vrushali Khobragade**[1], **Ting Yuan**[1], **Thomas Frogne**[2], **Wufan Tao**[3], **Jose Oberholzer**[4], **Francois Pattou**[5], **Julie Kerr Conte**[5], and **Kathrin Maedler**[1]

[1]Centre for Biomolecular Interactions Bremen, University of Bremen, Germany

[2]Department of Beta-cell Regeneration, Hagedorn Research Institute, Gentofte, Denmark

[3]Institute of Developmental Biology and Molecular Medicine, Fudan University, Shanghai, China

[4]Division of Transplantation, University of Illinois at Chicago, IL, USA

[5]Thérapie Cellulaire du Diabète, INSERM /Université de Lille Nord de France, France

[#] These authors contributed equally to this work.

Abstract

Apoptotic cell death is a hallmark of the loss of insulin producing beta-cells in all forms of diabetes mellitus. Current treatment fails to halt the decline in functional beta-cell mass. Strategies to prevent beta-cell apoptosis and dysfunction are urgently needed. Here, we identified Mammalian Sterile 20-like kinase 1 (MST1) as a critical regulator of apoptotic beta-cell death and function. MST1 was strongly activated in beta-cells under diabetogenic conditions and correlated with beta-cell apoptosis. MST1 specifically induced the mitochondrial-dependent pathway of apoptosis in beta-cells through up-regulation of the BH3-only protein Bim. MST1 directly phosphorylated PDX1 at Thr11, resulting in its ubiquitination, degradation and impaired insulin secretion. Mst1 deficiency completely restored normoglycemia, beta-cell function and survival *in vitro* and *in vivo*. We show MST1 as novel pro-apoptotic kinase and key mediator of apoptotic signaling and beta-cell dysfunction, which may serve as target for the development of novel therapies for diabetes.

Keywords

MST1; apoptosis; diabetes; beta-cells; pancreas

Pancreatic beta-cell death is the fundamental cause of type 1 diabetes (T1D) and a contributing factor to the reduced beta-cell mass in type 2 diabetes (T2D) [1-4]. In both cases

Contact: Kathrin Maedler, Ph.D. & Amin Ardestani, Ph.D., Islet Biology Laboratory, Centre for Biomolecular Interactions Bremen, University of Bremen, Leobener Straße NW2, Room B2080, 28359 Bremen, Germany, phone: +49(421)218-63290, Fax: +49(421)218-4279, kmaedler@uni-bremen.de/ ardestani.amin@gmail.com.

Authors' contribution:

- Conceived the project, designed all and performed most of experiments, analyzed the data and wrote the paper: AA
- Experimental and technical support and analyzed data: FP
- Performed experiments and analyzed data: ZA, SK, VK, TY
- Contributed new reagents or analytic tools: TF, WT, JKC, FP, JO
- Supervised the project and wrote the paper: KM

Detailed methods are given in the Supplementary material.

Europe PMC Funders Author Manuscripts

the mechanisms of beta-cell death are complex and as yet not fully defined. Thus, multiple triggering factors have been identified, which initiate a variety of signaling cascades that affect the expression of apoptotic genes and subsequent beta-cell failure. In T1D, autoimmune destruction of insulin-producing beta-cells and critically diminished beta-cell mass are hallmarks of the disease [2]. Beta-cell destruction occurs through immune mediated processes; mononuclear cell infiltration in the pancreatic islets and interaction between antigen presenting cells and T-cells leads to high local concentrations of inflammatory cytokines, chemokines, reactive oxygen species (ROS) and other apoptotic triggers (e.g. the perforin and Fas/FasL system) [2]. In T2D, beta-cell dysfunction and reduced beta-cell mass are the ultimate events leading to the development of clinically overt disease in insulin resistant individuals. Beta-cell destruction is caused by multiple stimuli including glucotoxicity, lipotoxicity, proinflammatory cytokines, endoplasmatic reticulum (ER) stress, and oxidative stress [5]. Unfortunately, none of the currently widely used anti-diabetic agents targets the maintenance of endogenous beta-cell mass, although it has been demonstrated that even a small amount of preserved endogenous insulin secretion has great benefits in terms of clinical outcome [6].

Beta-cells are highly sensitive to apoptotic damages induced by multiple stressors such as inflammatory and oxidative assault, due at least in part to their low expression of cytoprotective enzymes [7]. The initial trigger of beta-cell death remain still unclear; it follows an orchestra of events, which makes the initiation of beta-cell death complex and its blockade difficult to successfully achieve *in vivo*. Therefore, the identification of a common key regulator of beta-cell apoptosis would thus offer a novel therapeutic target for the treatment of diabetes.

The identification of the genes that regulate apoptosis has laid the foundation for the discovery of novel drug targets. Mammalian Sterile-20-like kinase (MST1, also known as STK4, KRS2) is an ubiquitously expressed serine/threonine kinase, it is part of the Hippo signaling pathway and involved in multiple cellular processes such as morphogenesis, proliferation, stress response and apoptosis [8,9]. MST1 is target as well as activator of caspases to amplify the apoptotic signaling pathway [10,11]. MST1 promotes cell death through regulation of multiple downstream targets such as LATS1/2, histone H2B, FOXO family members as well as induction of stress kinase c-Jun-N-terminal Kinase (JNK) and caspase-3 activation [9,12,13].

Genetic mutations and/or metabolic disturbances can alter protein networks and thereby disrupt downstream signaling pathways that are essential for beta-cell survival and function. Transcription factor PDX1 (pancreatic duodenal homeobox-1, previously called IPF1, IDX1, STF1, or IUF1) [14,15] is a key factor in beta-cell development and function [16]. In humans, mutations in PDX1 gene can predispose individuals to develop maturity onset diabetes of the young (MODY4) [17], suggesting that a critical role for PDX1 in mature beta-cells. Reduced PDX1 expression affects insulin production and secretion and predisposes to beta-cell apoptosis [16,18].

Since MST1 acts as common mediator in multiple apoptotic signaling pathways, we hypothesized that MST1 is an initiating trigger of apoptotic signaling in the beta-cell. MST1 depletion completely restored normogylcemia and insulin secretion and prevented diabetes progression. This makes MST1 as a fundamental novel target for diabetes therapy.

RESULTS

MST1 is activated in diabetes

To identify MST1 activation and its correlation with beta-cell apoptosis, we exposed isolated human and mouse islets and the beta-cell line INS-1E to a complex diabetic milieu *in vitro* (cytokine mixture IL-1β/IFNγ:IL/IF, increasing glucose concentrations, palmitic acid and oxidative stress: H_2O_2). MST1 was highly up-regulated by all diabetic conditions upon chronic exposure (Fig. 1a-c and Supplementary Fig. 1a,b) in beta-cells, which occurred by both caspase-mediated cleavage and through auto-phosphorylation (pMST1-T183). This was accompanied by higher phosphorylation of histone H2B as well as induction of c-jun N-terminal kinase (JNK) signaling (Fig. 1a-c). In contrast, short-term culture with elevated glucose did neither induce apoptosis nor MST1 cleavage and phosphorylation (Supplementary Fig. 1d). MST1 was also activated in islets from T2D subjects (Fig. 1d), obese diabetic $Lepr^{db/db}$ mice (db/db, Fig. 1e) and from hyperglycemic high fat/ high sucrose fed mice for 16 weeks (HFD; Surwit, Supplementary Fig. 1c), which correlated with beta-cell apoptosis as described before [19]. To confirm the beta-cell specific up-regulation of MST1, double-staining for pMST1 and insulin in pancreatic islets from poorly controlled subjects with T2D (Fig. 1d) as well as db/db mice (Fig. 1e) showed expression of pMST1 in beta-cells, while no signal was observed in non-diabetic subjects and control mice.

Caspase-3 and JNK act not only as downstream targets, but also as upstream activators of MST1 through cleavage- and phosphorylation-dependent mechanisms [12,20] and may initiate a vicious cycle and a pro-apoptotic signaling cascade in the beta-cell. Using JNK (SP600125) and caspase (z-DEVD-fmk) inhibitors and siRNA to caspase-3 (si*Casp3*), we found that both JNK and caspase-3 were responsible for stress-induced MST1 cleavage by diabetic stimuli in human islets and INS-1E cells (Supplementary Fig. 1e-h), suggesting that MST1 induces a positive feedback loop with caspase-3 under diabetogenic conditions. Because phosphatidylinositol-3 kinase (PI3K)/AKT signaling is a key regulator of beta-cell survival and function [21,22] and since MST1 signaling is negatively regulated by this pathway in other cell types [23,24], we hypothesized that AKT is an important negative regulator of MST1. Maintaining AKT-activation through either exogenously added mitogens like glucagon-like peptide 1 (GLP1) or insulin or overexpression of constitutively active AKT1 (Myr-AKT1) inhibited glucose- and cytokine-induced pMST1, MST1-cleavage and apoptosis (Fig. 1f and Supplementary Fig. 2a-d). Since GLP-1 and insulin exert their cell survival actions primarily through the PI3K/AKT pathway [21,25], we tested whether inhibition of this pro-survival signaling might enhance MST1 activation. PI3K and AKT were inhibited by LY294002 and triciribine (AKT inhibitor) led to lower levels of phosphorylation of GSK3 and FOXO1, two well-characterized AKT substrates and induced MST1 activation (Fig. 1g,h and Supplementary Fig. 2e). This was further corroborated using siRNA against AKT, which led to a critical up-regulation of MST1 activity and potentiated cytokine-induced PMST1 and beta-cell death (Supplementary Fig. 2f), also shown by diminished insulin-induced AKT phosphorylation in the presence of MST1; and conversely by enhanced AKT phosphorylation in MST1-depleted beta-cells (Fig. 1i). Knockdown of MST1 antagonized the apoptotic effect of AKT inactivation in INS-1E cells, implicating endogenous MST1 in the apoptotic mechanism induced by PI3K/AKT inhibition (Supplementary Fig. 2g,h). In summary, these results suggest that MST1 is activated in pro-diabetic conditions *in vitro* and *in vivo,* that is antagonized by PI3K/AKT signaling and depends on the JNK- and caspase-induced apoptotic machinery.

MST1 induces beta-cell death

MST1 overexpression was also itself sufficient to induce apoptosis in human and rodent beta-cells (Fig. 2a-c). To investigate pathways that potentially contribute to MST1-induced

beta-cell apoptosis, we overexpressed MST1 in human islets and INS-1E cells through an adenoviral system, which efficiently up-regulated MST1, induced beta-cell apoptosis and activated JNK, PARP- and caspase-3 cleavage (Fig. 2a-c). Previous data proposed a role of the mitochondrial pathway in MST-dependent signaling [26,27]. Profiling expression of established mitochondrial proteins in MST1-overexpressing islets showed cleavage of the initiator caspase-9, release of cytochrome *c,* induction of pro-apoptotic Bax and a decline in anti-apoptotic Bcl-2 and Bcl-xL levels (Fig. 2b-c and Supplementary Fig. 3a), which led to a reduction of Bcl-2/Bax and Bcl-xL/Bax. Notably, MST1-induced caspase-3 cleavage was reduced by treatment of human islets with the Bax-inhibitory peptide V5 (Fig. 2d), which was shown to promote beta-cell survival [28] and emphasizes that MST1-induced apoptosis proceeds via the mitochondrial-dependent pathway. We also analyzed the expression of BH3-only proteins as regulators of the intrinsic cell death pathway [29]. Of these, BIM was robustly induced, whereas other BH3-only proteins levels remained unchanged (Fig. 2b-c and Supplementary Fig. 3b). To assess whether kinase activity of MST1 is required for altering mitochondrial-dependent proteins and induction of apoptosis, we overexpressed kinase dead mutant of MST1 (K59R; dnMST1[30]) in human islets. Unlike wild-type MST1, dn-MST1 did not change the levels of BIM, BAX, BCL-2, BCL-xL and caspase-3 cleavage (Supplementary Fig. 3c). We next determined whether BIM is a major molecule to take over the pro-apoptotic action of MST1. Indeed, BIM depletion led to a significant reduction of MST1-induced apoptosis in human islets (Fig. 2e,f). Overexpression of MST1 further potentiated glucose-induced apoptosis in beta-cells in a BIM-dependent manner (Supplementary Fig. 3d). BIM is regulated by the JNK [31] and AKT [32] signaling pathways. MST1-induced increase in BIM and subsequent caspase-3 cleavage was prevented by JNK inhibition using two strategies; overexpression of dn-JNK1 (Fig. 2g) and pharmacological JNK inhibition (Supplementary Fig. 3e) suggesting that MST1 uses JNK signaling to mediate Bim upregulation and induction of apoptosis. The involvement of AKT in the regulation of MST1-induced apoptosis was confirmed by co-overexpression of MST1 and Myr-AKT1, which reduced BIM induction and caspase-3 cleavage (Fig. 2h), indicating that AKT negatively regulates the downstream target of MST1. These data suggest that MST1 is a critical mediator of beta-cell apoptosis through activation of the Bim-dependent intrinsic apoptotic pathway and controlled by AKT- and JNK signaling pathways.

MST1 impairs beta-cell function by destabilizing PDX1

We hypothesized that MST1 activation may elicit changes in beta-cell specific gene transcription that initiate the process of beta-cell failure. Overexpression of MST1 led to a complete loss of glucose-stimulated insulin secretion (GSIS; Fig. 3a and Supplementary Fig. 4a), which could not be accounted solely by the induction of apoptosis. Previously, we noted that the critical beta-cell transcription factor pancreatic duodenal homeobox-1 (PDX1), which mediates glucose-induced insulin gene transcription in mature beta-cells [16,18], is mislocalized and reduced in diabetes [19]. These changes are subsequently associated with impaired beta-cell function and hyperglycemia. Stress-induced kinases such as JNK and glycogen synthase kinase-3 (GSK3) phosphorylate and antagonize PDX1 activity [33,34], leading to beta-cell failure. Thus, we hypothesized that the drastic reduction in insulin secretion following MST1 overexpression may be mediated by PDX1. PDX1 levels were markedly reduced in response to MST1 overexpression in human islets (Fig. 3b) and INS-1E cells (Supplementary Fig. 4b). In contrast, MST1 overexpression did not affect the level of mRNA encoding PDX1 (Fig. 3b and Supplementary Fig. 4b), suggesting that MST1 may regulate PDX1 at the post-transcriptional level. Analysis of *PDX1* target genes demonstrated that overexpression of MST1 significantly down-regulated *Insulin* (*Ins1* or *Ins2* for INS-1E), *SLC2A2* and *GCK* in human islets (Fig. 3b) and INS-1E cells (Supplementary Fig. 4b). *SLC2A2*, although not the predominant glucose transporter in human beta-cells [35], was analyzed to provide comparison to the mouse data. To get a better insight into the role of

MST1 in regulation of insulin secretion, we have performed GSIS using two insulin secretagogues: GLP-1 and glibenclamide. MST1 overexpression significantly abolished GLP-1-enhanced glucose-induced insulin secretion, while glibenclamide-induced insulin secretion was not affected, suggesting that defective insulin secretion may occur at a step upstream of calcium influx (Supplementary Fig. 4c). MST1 overexpression had no effect on insulin content, thus insulin secretion was normalized on insulin content.

To clarify the mechanism by which MST1 regulates PDX1, we examined the effects of ectopic expression of MST1 and PDX1 in HEK293 cells. Lower PDX1 levels were found in cells co-overexpressing MST1, whereas a kinase-dead MST1 had no effect (Fig. 3c). Thus, kinase activity is required for MST1-induced PDX1 degradation. Overexpression of MST1 also attenuated the transcriptional activity of PDX1 on the rat insulin promoter, as shown by luciferase assays in PDX1 overexpressing HEK293 and INS-1E cells (Supplementary Fig. 4d). To discriminate between a transcriptional/translational and a post-translational effect of MST1 on PDX1, we followed the stability of overexpressed PDX1 upon treatment with cycloheximide (CHX), an inhibitor of protein translation. PDX1 protein levels rapidly decreased when co-expressed with MST1 upon CHX exposure (Fig. 3c), which suggests that MST1 reduced PDX1 protein stability. Consistent with these observations, MST1 overexpression also decreased protein stability of endogenous PDX1 in human islets (Supplementary Fig. 4e). In contrast, inhibition of proteasomal degradation by treatment of PDX1 overexpressing HEK293 cells with the proteasome inhibitor MG-132 reduced the disappearance of PDX1 (Fig. 3c), indicating that MST1-induced activation of the ubiquitin proteasome pathway. Proteasomal degradation of PDX1 has been described before and leads to impaired beta-cell function and survival [36]. *In vivo* ubiquitination assays were next performed to determine whether MST1 induces PDX1 ubiquitination. PDX1 co-transfected with MST1 but not with MST1-K59 was heavily ubiquitinated in HEK293 cells. This was confirmed in human islets by showing that MST1 overexpression strongly promoted endogenous PDX1 ubiquitination (Fig. 3d). Subsequently, a direct interaction between PDX1 and MST1 proteins was verified. Reciprocal co-immunoprecipitations showed the interaction between MST1 and PDX1 in HEK293 cells co-transfected with GFP-tagged PDX1 and myc-tagged MST1 (Fig. 3e). We next examined whether a pro-diabetic *milieu* regulates the association between MST1 and PDX1. Strikingly, both cytokine- and glucotoxicity augments the interaction between MST1 and PDX1 in INS-1E cells (Supplementary Fig. 4e). Since we observed that PDX1 ubiquitination and degradation required MST1 kinase activity, we tested whether MST1 directly phosphorylates PDX1. *In vitro* kinase assays showed that MST1 efficiently phosphorylated PDX1 shown by autoradiography using radiolabeled ^{32}P (Supplementary Fig. 4f) and by non-radioactive kinase assays and western blotting using a phospho-specific PDX1 antibody (Fig. 3f). The *in vitro* kinase assays were confirmed in HEK293 cells; co-expression of MST1 and PDX1 led to PDX1 phosphorylation (Supplementary Fig. 4f). Together, these results establish PDX1 as a substrate for MST1. The potential MST1-targeted phosphorylation sites of PDX1 were determined theoretically with the Netphos 2.0 program [37]. This identified six candidate sites including T11, T126, T152, T155, T214 and T231 within the PDX1 sequence based on a relative score (Supplementary Fig. 4g). These 6 sites were individually mutated to alanine to generate phospho-deficient constructs [38]. PDX1-GST fusion proteins with different PDX1 mutations were purified from bacteria and used as substrates for MST1 in the kinase assay. With the exception of T11A, PDX1-WT and other mutants were efficiently threonine phosphorylated (Supplementary Fig. 4h). To confirm this, all PDX1 mutants were transfected into HEK293 cells, immunoprecipitated with PDX1 and incubated with recombinant MST1 in a kinase assay. MST1 highly phosphorylated WT-PDX1 and other mutants, while phosphorylation in the PDX1-T11A was markedly lower (data not shown), indicating that T11 is major site of phosphorylation by MST1. To further validate this, a phosphospecific antibody against T11 phosphorylation site in PDX1 (p-T11PDX1)

recognized wild-type recombinant PDX1, which was incubated with MST1 in the kinase assay (Supplementary Fig. 4h). Consistently, co-incubation of immunoprecipitated PDX1-WT or PDX1-T11A with recombinant MST1 resulted in robust MST1-induced PDX1-WT phosphorylation at the T11 site (shown by p-T11 antibody) and in overall Thr-phosphorylation (shown by pan-Threonine antibody); such phosphorylation was markedly reduced in the PDX1-T11A mutant protein (Fig. 3g). This was further corroborated by an *in vivo* kinase assay (Supplementary Fig. 4h). Alignment of the amino acid sequences of PDX1 from different species revealed that T11 site is highly conserved among those species (Supplementary Fig. 4i). If T11 is the specific MST1-induced phosphorylation site of PDX1 and responsible for beta-cell dysfunction, one would expect that mutated PDX1-T11A would reverse such deleterious effects of MST1. This hypothesis was supported by the observation that MST1 did not lower PDX1 levels in PDX1-T11A-expressing HEK293 cells. MST1 induced a rapid degradation of PDX1 in the presence of CHX, which did not occur in PDX1-T11A mutant transfected cells (Fig. 3g). Furthermore, the half-life of the PDX1-T11A mutant was similar as PDX1-WT in the absence of MST1 (data not shown). Consistently, there was less PDX1 ubiquitination in the PDX1-T11A-transfected cells than in PDX1-WT (Supplementary Fig. 4j). Since T11 is located within the transactivational domain of PDX1 and to evaluate the functional significance of the T11-dependent ubiquitination/degradation, we assessed transcriptional activity of PDX1. Reduction of PDX1 transcriptional activity occurred only in PDX1-WT but not in PDX1-T11A mutant transfected cells (Supplementary Fig. 4j). Since mutation of PDX1 on T11 prolongs PDX1 stability, we asked whether PDX1 stability is directly linked to improved beta-cell function. Indeed, PDX1-T11A mutant overexpression (Fig. 3h) normalized MST1-induced impairment in GSIS in human islets (Fig. 3i) and INS-1E cells and restored MST1-induced down regulation of PDX1 target genes (Fig. 3j and Supplementary Fig. 4j). These findings indicate that MST1-induced PDX1 phosphorylation at T11 leads directly to PDX1 de-stabilization and impaired beta-cell function and suggest that PDX1 is a crucial target of MST1 in the regulation of beta-cell function.

MST1 deficiency improves beta-cell survival and function

Our further analyses established MST1 as a master regulator of apoptosis in beta-cells. MST1 not only mediated beta-cell death and impaired function *in vitro*, but its down-regulation could rescue from beta-cell failure (Fig. 4 and Supplementary Fig. 5). Firstly, about 80% depletion of MST1 in human achieved by siRNA protected from cytokine-, H_2O_2-, glucolipo-toxicity; beta-cell apoptosis was inhibited (Fig. 4a,b and Supplementary Fig. 5a). Silencing of MST1 also significantly reduced BIM upregulation induced by diabetogenic conditions in human islets (Fig. 4b,c and Supplementary Fig. 5a).

Secondly, beta-cell function was greatly improved by *MST1* gene silencing under diabetogenic conditions (Fig. 4d and Supplementary Fig. 5). Notably, IL/IF- and HG/Pal-induced caspase-3 and -9 cleavage and PH2B was all lower in MST1-depleted human islets, compared to control islets (Fig. 4b). *Mst1*$^{-/-}$ islets largely resisted to IL/IF- and HG/Pal-mediated apoptosis as determined by TUNEL staining (Fig. 4e). In addition to the protective effect on beta-cell survival, *Mst1*$^{-/-}$ islets also showed improved GSIS after long-term culture with IL/IF and HG/Pal (Fig. 4f and Supplementary Fig. 5). To further support the role of MST1 as a main mediator of apoptosis in the beta-cells, we generated INS-1E cells stably transfected with vector for shScr and shMST1 and confirmed an about 70% reduction in MST1 expression of the cells stably expressing shMST1 (Fig. 4g). INS-1E clones were treated with IL/IF and HG for 72 hours. Bim induction, caspase-3- and PARP- cleavage in MST1-depleted cells was significantly lower compared to control cells (Fig. 4g). Additionally, MST1 silencing also abrogated caspase-3 and PARP cleavage induced by palmitate (Supplementary Fig. 5b) and H_2O_2 (Supplementary Fig. 5c). Cytochrome *c* release

was markedly reduced in MST1-depleted beta-cells under diabetogenic conditions (Supplementary Fig. 5d,e). A second shRNA clone to the MST1 gene with comparable gene silencing efficiency confirmed the anti-apoptotic effect of MST1 silencing in INS-1E cells; MST1 depletion markedly suppressed IL/IF- and HG-induced Bim up-regulation and cleavage of caspase-3 and PARP (Supplementary Fig. 5f). In confirmation with the shMST1 approach, we show that inhibition of endogenous MST1 activity by overexpression of dn-MST1 completely inhibited glucose-induced caspase-3 and PARP cleavage in beta-cells (Supplementary Fig. 5g).

MST1 deficiency significantly attenuated PDX1 depletion upon cytokine and high glucose treatment, implying that MST1 is indispensable for the PDX1 reduction induced by a diabetic milieu (Fig. 4g and Supplementary Fig. 5f). Our next objective was to determine whether MST1 knockdown leads to improvement of GSIS and restoration of PDX1 target genes in INS-1E cells under diabetogenic conditions. GSIS was significantly improved in MST1 depleted beta-cells (Fig. 4h and Supplementary Fig. 5j), while levels of PDX1 target genes, e.g. *SLC2A2, GCK, Ins1* and *Ins2* were restored in MST1-depleted INS-1E cells (Fig. 4i). These data prove MST1 as determinant for beta-cell apoptosis and defective insulin secretion under a diabetic milieu in beta-cells *in vitro*.

Mst1 deletion protects from MLD-STZ-induced diabetes

Since MST1 depletion protected from beta-cell apoptosis and restored beta-cell function *in vitro*, we hypothesized that Mst1 deficiency may protect against diabetes *in vivo* by promoting beta-cell survival and preserving beta-cell mass. To test this hypothesis, we used *Mst1*$^{-/-}$ mice. Neither body weight nor food intake differed between *Mst1*$^{-/-}$ and their wild-type littermates (*Mst1*$^{+/+}$; WT) mice (data not shown). Also, glucose tolerance, insulin tolerance and glucose-induced insulin response did not differ between WT and *Mst1*$^{-/-}$ mice at 2 months of age (Supplementary Fig. 6a). However, IPGTT and IPITT tests revealed slight improvement in *Mst1*$^{-/-}$ mice at 6 months of age at 60 min after glucose/ insulin injection (Supplementary Fig. 6b). Diabetes was induced by multiple low-dose streptozotocin (MLD-STZ) injections in *Mst1*$^{-/-}$ and their wild type controls. While progressive hyperglycemia and severely impaired glucose tolerance was induced in WT mice by MLD-STZ injections, blood glucose levels were significantly reduced and ipGTT highly improved in *Mst1*$^{-/-}$ mice (Fig. 5a). The MLD-STZ treatment led to impaired insulin secretion and insulin to glucose ratio in WT mice, which was significantly restored in *Mst1*$^{-/-}$ mice (Fig. 5b,c). Islet architecture in STZ-treated WT mice was disrupted and accompanied by less insulin staining, beta-cell fraction, islet density, islet size and beta-cell mass compared to that of non-MLD-STZ-treated mice. In contrast, islet architecture of MLD-STZ-*Mst1*$^{-/-}$ mice had a close-to-normal appearance and beta-cell fraction, islet density and beta-cell mass was similar to non-MLD-STZ-treated mice (Fig. 5d,e and Supplementary Fig. 6c). Islet size also tended to be higher in MLD-STZ-injected *Mst1*$^{-/-}$ mice than in WT mice, although this effect was not statistically significant (Supplementary Fig. 6c). To elucidate how MST1 deletion may affect beta-cell mass, we studied beta-cell apoptosis and proliferation. TUNEL staining demonstrated that apoptosis was dramatically higher in STZ-treated WT mice. *Mst1* deletion in *Mst1*$^{-/-}$ mice markedly lowered apoptosis. Beta-cell proliferation was higher in MLD-STZ compared to WT mice but *Mst1*$^{-/-}$ beta-cells showed even higher proliferation, indicative of an improved compensatory capacity (Fig. 5d and Supplementary Fig. 6d,e). No difference in the frequency of proliferating beta-cells was observed between islets from *Mst1*$^{-/-}$ mice and their WT littermates at basal levels. These results suggest that *Mst1* deletion boosts beta-cell mass and islet density predominantly as a result of lower beta-cell apoptosis and higher beta-cell proliferation in response to diabetogenic stimulation. To further assess the effect of MLD-STZ, immunohistochemical analyses for insulin and glucagon were performed on pancreatic

sections. Islet cells from MLD-STZ-treated WT mice were architecturally distorted, containing significantly fewer insulin-positive cells and proportionally more glucagon-positive cells result in alpha-cell to beta-cell ratio (Fig. 5e). This is consistent with previously reported alpha-cell hyperplasia in diabetes [39,40]. In contrast, number of glucagon-positive alpha-cells was not higher and confined to the rim of the islets, suggesting that the architecture of MLD-STZ-injected *Mst1*$^{-/-}$ islets was close to normal (Fig. 5e). In line with our *in vitro* results in beta-cells, where MST1 acts through changes in Bim, expression of the latter was clearly seen in beta-cells in diabetic STZ-mice, but not in *Mst1*$^{-/-}$ mice (Fig. 5f). We next examined Pdx1 expression as beta-cell-specific MST1 substrate, which is regulated by both its abundance and its sub-cellular localization in diabetic conditions [19]. While MLD-STZ- treated WT showed a markedly higher total amount and nuclear localization of Pdx1 in beta-cells, Pdx1-expression was normalized and the prominent nuclear localization important for its functionality re-established in MLD-STZ-treated *Mst1*$^{-/-}$ mice (Fig. 5g). The Pdx1 target gene Glut2 was largely preserved in beta-cell membranes in the MLD-STZ-treated *Mst1*$^{-/-}$ mice, while it was barely detectable in the MLD-STZ- treated WT mice (Supplementary Fig. 6f). These findings suggest that *Mst1* deletion preserves Pdx1 and Glut2 membrane localization in beta-cell membranes and thus preserves the function of beta-cells in this model of diabetes. To directly assess the protective effect of *Mst1* deletion in STZ-induced beta-cell apoptosis, we treated isolated mouse islets and INS-1E cells with STZ *in vitro* and found that STZ strongly induced pMst1, Bim and ultimately apoptosis, and such apoptotic induction by STZ was attenuated by Mst1 depletion (Supplementary Fig. 6g,h), consistent with the *in vivo* observations in *Mst1*$^{-/-}$ mice.

To exclude a secondary effect of the *Mst1*-deletion on the beta-cell, beta-cell-specific *Mst1*$^{-/-}$ mice were generated by the Cre-lox system (hereafter referred to as b*Mst1*$^{-/-}$ mice). Mice contained a null mutation for *Mst1*, as confirmed by western blotting of lysates from isolated islets (Supplementary Fig. 7a). b*Mst1*$^{-/-}$ mice were viable, fertile and showed no difference in food intake and body weight (data not shown), glucose tolerance and insulin sensitivity compared to *Mst1*$^{fl/fl}$ (Supplementary Fig. 7b,c) or flox-negative littermates (RIP-*Cre*; data not shown). To assess whether b*Mst1*$^{-/-}$ mice might also be protected against diabetes, we again used the model of MLD-STZ-induced diabetes. After MLD-STZ treatment, blood glucose levels in *Mst1*$^{fl/fl}$ and RIP-*Cre* control mice increased gradually (Fig. 5h). While both control groups became overtly diabetic, reaching blood glucose levels >400 mg/dl, b*Mst1*$^{-/-}$ mice maintained normal blood glucose levels. *Mst1*$^{fl/fl}$ and RIP-*Cre* control mice exhibited impaired glucose tolerance; this was strikingly improved in b*Mst1*$^{-/-}$ mice (Fig. 5h). This protection was accompanied by significant restoration of glucose-induced insulin response and insulin/glucose ratio (Fig. 5i). Beta-cell protection was also confirmed by the considerably higher beta-cell mass in the MLD-STZ-b*MST1*$^{-/-}$ mice resulting from enhanced beta-cell survival and proliferation (Fig. 5j), compared *to Mst1*$^{fl/fl}$ and RIP-*Cre* control mice. These data indicate that beta-cell-specific disruption of *Mst1* prevented progressive hyperglycemia and improved glucose tolerance in MLD-STZ-treated mice as a result of lesser apoptosis and restoration of beta-cell mass suggesting that beta-cell-specific activation of Mst1 is a key event in the progressive loss of beta-cells in diabetes.

Mst1 deletion protects from high-fat diet induced diabetes

The protective effect of *Mst1* deletion against hyperglycemia and development of diabetes was further confirmed in a mouse model of T2D. b*Mst1*$^{-/-}$ mice and their Rip-*Cre* controls were fed a normal (ND) or a high fat/ high sucrose diet (HFD) for 20 weeks. Mice fed HFD gained more weight than the ND group. Beta-cell-specific disruption of *Mst1* had neither an effect on weight gain nor food intake in both groups (Supplementary Fig. 7d,e). High fat feeding increased fed and fasted glucose levels (Fig. 6a,b) and impaired glucose tolerance

(Fig. 6b) in the HFD-treated RIP-*Cre* control mice compared to ND, whereas HFD-treated b*Mst1*$^{-/-}$ mice showed significantly lower fed and fasted glucose as well as improved glucose tolerance (Fig. 6a,b).

In RIP-*Cre* mice on HFD, insulin secretion during i.p. glucose challenge was markedly attenuated compared with its ND group. In contrast, HFD-induced impairment in GSIS was dramatically reversed by the beta-cell specific deletion of *Mst1* (Fig. 6c). For assessing beta-cell glucose responsiveness, islets were isolated from all ND and HFD groups. While GSIS was severely impaired in islets isolated from HFD-treated RIP-*Cre* mice compared with ND-treated RIP-*Cre* mice, islets from b*Mst1*$^{-/-}$ mice remained fully glucose responsive with improved insulin secretion (Fig. 6d). Consistent with the improved metabolic phenotype of b*Mst1*$^{-/-}$ mice on HFD, b*Mst1*$^{-/-}$ mice had a higher compensatory beta-cell mass relative to control mice (Fig. 6e). The combination of lower beta-cell apoptosis and elevated beta-cell proliferation (Fig. 6e) in b*Mst1*$^{-/-}$ mice on the HFD, which accounts for the higher beta-cell mass in b*MST1*$^{-/-}$ mice, correlates with the improved glucose tolerance and insulin secretion. This is also supported by results from an ipITT; then glucose levels were normalized to the basal levels before insulin injection, both b*MST1*$^{-/-}$ mice and RIP-*Cre* control mice on HFD showed a similar impairment in insulin sensitivity (Supplementary Fig. 7f,g).

To test whether MST1 knockdown could directly rescue diabetic beta-cells, islets isolated from 10-week old obese db/db mice and their db/+ littermate controls were transfected with siScr or siMst1. While siScr treated isolated db/db islets showed low Pdx1, high caspase-3 cleavage and Bim expression, Mst1 silencing restored Pdx1, inhibited Bim up-regulation and dramatically reduced caspase-3 cleavage (Supplementary Fig. 8).

DISCUSSION

Our work shows that MST1 acts as an essential apoptotic molecule in the presence of diabetic stimuli and is a common component in the diverse signaling pathways leading to impaired beta-cell survival in diabetes. We identified PDX1 as novel and beta-cell specific substrate for MST1. PDX1 ubiquitination and subsequent degradation, resulting from inhibitory T11 phosphorylation, is crucial for beta-cell dysfunction after MST1 hyper-activation in diabetes (Fig. 6i). Deletion of *Mst1* preserves beta-cell function and survival providing protection from diabetic insults.

MST1 plays a central role in the initiation of cell death [9,41-44]. In line with our data, *Mst1* ablation *in vivo* resulted in resistance to TNF-α- [45] Fas ligand- [46] and IFN-γ- [47] induced apoptosis. Remarkably, suppression of endogenous Mst1 by cardiac-specific overexpression of the dominant-negative form of MST1 prevented cardiomyocyte death induced by ischemia/ reperfusion [48] supporting the patho-physiological significance of MST1. The complexity of diabetic stimuli by which MST1 is activated in beta-cells, suggests that this enzyme may be a common component in the diverse signaling pathways leading to beta-cell apoptosis. While the endogenous molecules, that trigger MST1 activation remain unknown, we show that MST1 is highly active in a diabetic environment and induces the mitochondrial-dependent apoptosis pathway in beta-cells through targeting Bim, which leads to alterations in Bax/Bcl-2, cytochrome *c* release, subsequent caspase-9 and -3 cleavage and cell death.

The PI3K/AKT pathway plays a critical role in the regulation of beta-cell survival. AKT-mediated phosphorylation of multiple substrates positively regulates insulin transcription, insulin secretion, and beta-cell growth and survival [21,22,49]. Recent studies suggest potential crosstalk between MST1 and AKT [23,24]. MST1 activity is negatively regulated by AKT-

mediated phosphorylation at its Thr120 and Thr387 residues and results in inhibition of its cleavage, autophosphorylation, kinase activity and nuclear translocation [23]. On the other hand, MST1 and its cleaved form interact with AKT1 and act as direct AKT1 inhibitors [24]. Our data demonstrate that activation of the PI3K-AKT pathway in beta-cells abrogate glucose- and cytokine-induced MST1 activation and beta-cell apoptosis, whereas suppression of PI3-K/AKT signaling induces MST1 activity and beta-cell apoptosis. AKT and MST1 are components of two parallel stress-triggered signaling pathways, which functionally antagonize each other. Activated AKT itself down-regulates MST1 function in the beta-cells, indicating the existence of a potential bidirectional crosstalk between these two pathways. Here we show that MST1 and AKT negatively regulate each other and constitute a stress-sensitive survival pathway. Under acute stress conditions, AKT promoted cell survival by inhibiting MST1, but prolonged stress decreased AKT, which allowed pro-apoptotic MST1 signaling.

MST1 may affect signal pathways of diabetic stimuli through modulation of transcription factors and gene expression profiles that initiate the process of beta-cell failure. In this study, we show that MST1 can physically interact with and phosphorylate PDX1. Targeted disruption of PDX1 in beta-cell leads to diabetes, and reducing its expression affects insulin expression and secretion [50]. We have identified threonine 11 (T11) residue of PDX1 as the phosphorylation site used by MST1. Such a kinase-dependent function would be consistent with a comparably low level of PDX1 and high levels of active MST1 in stressed beta-cells and pancreases of diabetic mice in our study. PDX1 is restored by MST1 knockdown in beta-cells and by deletion of *Mst1* in knockout mice under diabetic conditions. This modified threonine is found in the highly conserved region of PDX1 at the transcription activation domain. T11-phosphorylation of PDX1 by MST1 marks PDX1 for degradation by the proteasome machinery, which would prohibit it to function as a transcription factor in the nucleus. In that regard, overexpression of MST1 causes reduction of PDX1 target genes and beta-cell functional impairment, as assessed by GSIS, whereas mutation of the T11 site allowed PDX1 to be more stabilized and resistant to a MST1-induced degradation to restore PDX1-induced gene expression and improvement of beta-cell function. The same site (Thr11) was previously shown to be targeted by DNA-dependent protein kinase. Consistent with our data, phosphorylation of PDX1 by this kinase results in enhanced protein degradation [51]. PDX1 is degraded by the ubiquitin-proteasome pathway; PDX1 C-terminus-interacting factor 1 (Pcif1) targets PDX1 for ubiquitination and proteasomal degradation by the E3 ubiquitin ligase Culin3. PDX1 ubiquitination regulates PDX1 activity since Pcif1 deficiency normalizes Pdx1 protein levels and improves glucose homeostasis and beta-cell function in *Pdx1*$^{+/-}$ mice [36]. Interestingly, accumulation of polyubiquinated proteins was higher in beta-cells of individuals with T2D [52] highlighting that higher expression of polyubiquinated proteins may contribute to beta-cell dysfunction under diabetic conditions.

In mammals, the absolute number of beta-cells reflects a dynamic balance between beta-cell growth and death. An inadequate expansion of beta-cell mass to compensate for the increased insulin demand, followed by the eventual loss of beta-cells due to apoptosis, is a hallmark of diabetes [4,53]. This is most apparent in T1D when ongoing autoimmunity causes destruction and consequent loss of beta-cells. Through deletion of the MST1-mediated death signal, we have uncovered an important deleterious action of MST1 to induce apoptosis in response to diabetic injuries in the immune-mediated beta-cell destruction in the MLD-STZ model, a model of beta-cell demise that occurs in the absence of insulin resistance. *Mst1* deletion not only prevents MLD-STZ-induced beta-cell death, but also improves the capacity of the beta-cell to produce insulin. *Mst1* deletion preserves beta-cell mass and improves beta-cell function and prevents islets deterioration, as shown by the maintenance of the islet structure, density, size and mass. The observed ability to preserve the islets

appearance is associated with a protective role of Mst1 deficiency on MLD-STZ-induced beta-cell death and enhancing beta-cell proliferation.

Preservation of PDX1 is one mechanism involved in the protection of beta-cells by MST1 depletion. This conclusion is strongly supported by our *in vitro* and *in vivo* data; Pdx1 target genes are normalized and Glut2 localization is preserved in *Mst1*$^{-/-}$ mice. Since both Pdx1 and Glut2 are involved in glucose sensing and glucose-stimulated insulin secretion, *Mst1*$^{-/-}$ mice show normal blood glucose levels and higher circulating insulin concentrations. STZ enters the beta-cells via Glut2. It is unlikely that resistance of *Mst1*$^{-/-}$ mice to STZ-induced beta-cell damage is due to changes in membrane Glut2 expression in beta-cells, because *Mst1* deletion did not reduce membrane expression of Glut2 in beta-cells in mice without STZ treatments.

The high rate of apoptosis in the Mst1-deficient thymocytes further illustrates the cell type-specific variation in the outputs of MST1 signaling. While in thymocytes and T-cells, deletion of *Mst1* increases the apoptosis rate [54-56] possibly through high levels of ROS; Mst1-deficient hepatocytes and microglia exhibit a marked resistance to stress-induced apoptosis [46,47]. Thus, the consequences of Mst1 deficiency needs to be established in each cell type and tissue. Tissue-specific gene-targeting approach was used in the current study to provide insights into the biological role of Mst1 in beta-cells *in vivo*. It is known that both T-cell and macrophage activation and migration play an important role in islet destruction leading to hyperglycemia in the MLD-STZ model [57]. Infiltrating macrophages and T-cells are a major source of the pro-inflammatory cytokines that promote islet destruction. Thus, the depletion of peripheral T-cells in *Mst1*$^{-/-}$ mice [54,55] might be a reason for their protection from MLD-STZ-induced hyperglycemia. We cannot exclude such T-cell depletion in our model, but if it occurs, it only plays a minor role, because beta-cell-specific deletion of *Mst1* completely protected from hyperglycemia and islet destruction. This shows that *Mst1* ablation in beta-cells and not in other tissues is a major reason for the protection from MLD-STZ induced diabetes. Importantly, beta-cell-specific deletion of *Mst1* in this model led to protection against beta-cell apoptosis and diabetes, further underlining the critical role beta-cell MST1 plays for beta-cell survival. Consistently, it should be noted that isolated islets from *Mst1*$^{-/-}$ mice are protected from STZ- and cytokine-induced apoptosis *in vitro*, further proving that protection of *MST1*$^{-/-}$ mice from islet destruction in the MLD-STZ model is due to intrinsic resistance of *Mst1*$^{-/-}$ beta-cells to stress-induced cytotoxicity.

The detrimental effects of a long-term high fat/ high sucrose diet on beta-cell function and insulin sensitivity leading to glucose intolerance and type 2 diabetes in mice have been clearly established [58]. As expected, long-term high-fat diet feeding was associated with insulin resistance, glucose intolerance, beta-cell dysfunction and loss of compensatory beta-cell adaptation. Similar to the effects in the MLD-STZ model, beta-cell specific *Mst1* deletion results in improved glucose tolerance, insulin secretion and beta-cell mass as a result of improved beta-cell survival and proliferation, while insulin sensitivity is not affected. Besides in beta-cells, we have not investigated whether Mst1 is also activated in other organs during diabetes progression, but activated Mst1 was also found in the kidney of hyperglycemic IRS2-KO mice [59] and in epididymal fat pads of HFD-treated mice [60].

Our findings raise the possibility that MST1 hyperactivity is associated with beta-cell failure and development of diabetes. Current therapies for the treatment of diabetes mellitus are directed towards alleviating the symptoms of the disease, but there is an urgent medical need for therapies that slow or prevent the loss (rapid in T1D, progressive in T2D) of functional pancreatic beta-cell mass. In light of the critical role of MST1 in beta-cell failure and initiation of “pro-diabetic milieu”-induced apoptotic signaling, therapeutic strategies

designed to inhibit MST1 activity may both protect the beta-cell against the effects of autoimmune attack in T1D and preserve beta-cell mass and function in T2D.

Online Methods

Cell culture, treatment and islet isolation

Human islets were isolated from twenty pancreases of healthy organ donors and from five with T2D at the University of Illinois at Chicago or Lille University and cultured on extracellular matrix (ECM) coated dishes (Novamed, Jerusalem, Israel) as described previously [61]. Islet purity was greater than 95% as judged by dithizone staining (if this degree of purity was not achieved by routine isolation, islets were handpicked). Islets from MST1$^{-/-}$ mice and their WT littermates were isolated as described previously [61]. Pancreata were perifused with a Liberase TM (#05401119001, Roche, Mannheim, Germany) solution according to the manufacturer's instructions and digested at 37°C, followed by washing and handpicking. The clonal rat beta-cell line INS-1E was kindly provided by Dr. Claes Wollheim, Geneva & Lund University. Human islets were cultured in complete CMRL-1066 (Invitrogen) medium at 5.5 mM glucose and mouse islets and INS-1E cells at complete RPMI-1640 medium at 11.1 mM glucose and HEK293 cells were cultured in Dulbecco's modified Eagle's medium (DMEM). All media included with glutamate, 1% penicillin-streptomycin and 10% fetal bovine serum (FBS, all PAA). INS-1E medium was supplemented with 10 mM HEPES, 1 mM sodium pyruvate and 50 μM β-mercaptoethanol. Islets and INS-1E were exposed to complex diabetogenic conditions: 22.2-33.3 mM glucose, 0.5 mM palmitic acid, the mixture of 2 ng/ml recombinant human IL-1β (R&D Systems, Minneapolis, MN) +1,000 U/ml recombinant human IFN-γ (PeProTech) for 72h, 100 μM H_2O_2 for 6h, 1 mM streptozotocin (STZ) for 8h or 1 mM thapsigargin for 6h (all Sigma). In some experiments, cells were additionally cultured with 10-25 μM JNK selective inhibitor SP600125, 25 μM selective PI-3 kinase inhibitor LY294002, 20 μM AKT inhibitor V, Triciribine, selective AKT1/2/3 inhibitor, 25 μM pan-caspase inhibitor Z-VAD (OMe)-fmk, 100 μM Bax-inhibiting peptide V5 or Bax-inhibiting peptide, negative control, InSolution™ MG-132, proteasome inhibitor (all Calbiochem), 100 nM Glucagon like-peptide 1 (GLP1), 100 nM recombinant human insulin, cycloheximide (CHX) and 1μM glibenclamide_(all Sigma). Palmitic acid was dissolved as described previously [62]. Ethical approval for the use of islets had been granted by the Ethics Committee of the University of Bremen.

Animals

For MLD-STZ experiment, 8-10 week old *Mst1*$^{-/-}$ mice on a 129/sv genetic background [55] and their *Mst1*$^{+/+}$ WT littermates were i.p. injected with streptozotocin (STZ; 40 mg/kg; Sigma) freshly dissolved in 50mM sodium citrate buffer (pH 4.5) or citrate buffer as control for 5 consecutive days (referred to as multiple low dose/MLD-STZ). To create beta-cell-specific *Mst1*$^{-/-}$ mice, mice harboring exon 4 of the *Mst1* gene flanked by *loxP* sites (*Mst1*$^{fl/fl}$) [55]) were crossed with mice expressing *cre* under the rat insulin-2 promoter (B6;D2-Tg(Ins-cre)23Herr: RIP-*Cre* [63], kindly provided by Pedro Herrera, University of Geneva and Ahmed Mansouri, Max Planck Institute for Biophysical Chemistry). RIP-*Cre*-*Mst1*$^{fl/-}$ mice were intercrossed to generate RIP-*Cre*-*Mst1*$^{fl/fl}$. Mice were MLD-STZ injected as described above. For the high fat diet (HFD) experiments, 8-week old RIP-*Cre*-*Mst1*$^{fl/fl}$ (b*Mst1*$^{-/-}$) mice and their Rip-*Cre* controls were fed a normal diet (ND, Harlan Teklad Rodent Diet 8604, containing 12.2, 57.6 and 30.2% calories from fat, carbohydrate and protein, respectively) or a high fat/ high sucrose diet (HFD, "Surwit" Research Diets, New Brunswick, NJ, containing 58, 26 and 16% calories from fat, carbohydrate and protein, respectively [58,64]) for 20 weeks. For both models, random blood was obtained from the tail vein of non-fasted mice and glucose was measured using a Glucometer (Freestyle; TheraSense Inc., Alameda, CA). Mice were killed at the end of experiment, pancreas was

Europe PMC Funders Author Manuscripts

isolated. Throughout the whole study, food consumption and body weight were measured weekly. Only male mice were used in the experiments. All animals were housed in a temperature-controlled room with a 12-hour light/dark cycle and were allowed free access to food and water in agreement to NIH animal care guidelines of the §8 German animal protection law and approved by the Bremen Senate.

Intraperitoneal glucose and insulin tolerance tests and measurement of insulin release

For intraperitoneal glucose tolerance tests (ipGTTs), mice were fasted 12h overnight and injected i.p. with glucose (40%; B.Braun, Melsungen, Germany) at a dose of 1 g/kg body weight. Blood samples were obtained at time points 0, 15, 30, 60, 90, and 120 min for glucose measurements using a Glucometer and at time points 0, 15 and 30 min for measurement of serum insulin levels. For i.p. insulin tolerance tests, mice were injected with 0.75 U/kg body weight recombinant human insulin (Novolin, Novo Nordisk) after 5-h fasting, and glucose concentration was determined with the Glucometer. Insulin secretion was measured before (0min) and after (15 and 30min) i.p. injection of glucose (2 g/kg) and measured using ultrasensitive mouse Elisa kit (ALPCO Diagnostics, Salem, NH).

Plasmids

pCMV-myc-MST1 and kinase-dead (MST1-K59; dnMST1) was kindly provided by Dr. Junichi Sadoshima and Dr. Yasuhiro Maejima (UMDNJ, New Jersey Medical School) [30]. Mouse pB.RSV.PDX1-GFP plasmid was kindly provided by Dr. Ingo Leibiger (Karolinska University, Stockholm). pcDNA3 Myr-HA Akt1, HA-Ubiquitin and pCDNA3 Jnk1a1 (apf) (dn-JNK) plasmids were obtained from Addgene (Cambridge, MA). Mouse PDX1 mutants (T11, T126, T152, T155, T214 and T231) in pCGIG5 vector were generated by site-directed mutagenesis as described previously [38]. All mutations were verified by sequencing. To make bacterial expression plasmids for PDX1 mutants, the complete mouse PDX1 CDS (wild type and mutants) has been amplified by PCR using a specific set of primers from pCGIG5 plasmids and cloned into a pGEX-6P-1 bacterial expression vector (kindly provided by Dr. Reinhard Walther, University of Greifswald). The rat insulin driven luciferase vector (RIP-Luc) was constructed by subcloning a 700bp fragment containing -660bp of the rat 2 insulin promoter (kindly provided by Dr. Rolf Zinkernagel, University of Zurich) into a pMCS-Green-Renilla-Luc vector (Thermo Scientific). pCMV-Red firefly Luc vector was obtained from Thermo Scientific.

Transfections

To knockdown MST1 in human islets, SMARTpool technology from Dharmacon was used. A mix of ON-TARGETplus siRNAs directed against the following sequences in human MST1: UAAAGAGACCGGCCAGAUU, GAUGGGCACUGUCCGAGUA, GCCCUCAUGUAGUCAAAUA, CCAGAGCUAUGGUCAGAUA and mouse MST1: GAUGGGCACUGUCCGAGUA, UGACAGCCCUCACGUAGUC, GCAGGUCAACUUACAGAUA, CUACAGCACCCGUUUGUUA (100 nM, Dharmacon) was transiently transfected into human and mouse islets and efficiently reduced MST1 levels. An ON-TARGETplus non-targeting siRNA pool from Dharmacon served as a control. To knock down Bim and caspase-3 in human islets, siRNA targeting human Bim (SignalSilence Bim SiRNA I, Cell Signaling) and caspase-3 (NEB) was used. GFP, MST1, dn-MST1 (K59), dn-JNK1 and Myr-Akt1 plasmids were used to overexpress these proteins in human islets and INS-1E cells.

An adapted improved protocol to achieve silencing and overexpression in human islets was developed [19,65]. Islets were partially dispersed with accutase (PAA) to break islets into smaller cell aggregates to increase transfection efficiency and cultured on ECM dishes for at least 2 days. Isolated islets and INS-1E cells were exposed to transfection Ca^{2+}-KRH

medium (KCl 4.74 mM, KH_2PO_4 1.19 mM, $MgCl_26H_2O$ 1.19 mM, NaCl 119 mM, $CaCl_2$ 2.54 mM, $NaHCO_3$ 25 mM, HEPES 10 mM). After 1h incubation, lipoplexes (Lipofectamine2000, Invitrogen)/-siRNA ratio 1:20 pmol or -DNA ratio 2.5:1) were added to transfect the islets and INS-1E cells. After additional 6h incubation, CMRL-1066 or RPMI-1640 medium containing 20% FCS and L-Glutamine were added to the transfected islets or INS-1E cells. Efficient transfection was evaluated based on Fluorescein-labeled siRNA (NEB) or eGFP positive cells analyzed by fluorescent or confocal microscopy. HEK293 were transiently transfected using Optimem medium and Lipofectamine (Invitrogen) according to the manufacturer's instructions.

Glucose stimulated insulin secretion

For acute insulin release in response to glucose, primary human and mouse islets and INS-1E cells were washed and pre-incubated (30 min) in Krebs-Ringer bicarbonate buffer (KRB) containing 2.8 mM glucose and 0.5% BSA. KRB was then replaced by KRB 2.8 mM glucose for 1 h (basal), followed by an additional 1 h in KRB 16.7 mM glucose with or without 100 nM GLP1 or 1μM glibenclamide. Insulin content was extracted with 0.18N HCl in 70% ethanol. Insulin was determined using human and mouse insulin ELISA (ALPCO Diagnostics, Salem, NH). Secreted insulin was normalized to insulin content.

Immunohistochemistry

Pancreatic tissues were processed as previously described [66]. In brief, mouse pancreases were dissected and fixed in 4% formaldehyde at 4°C for 12h before embedding in paraffin. Human and mouse 4-μm sections were deparaffinized, rehydrated and incubated overnight at 4°C with anti-insulin (Dako), anti-P-MST1 (Cell Signaling), anti-Bim (Cell Signaling), anti-PDX-1 (abcam), anti-glucagon (Dako), anti-glut2 (Chemicon) and anti-mouse anti-Ki67 (BD Pharmingen) antibodies followed by fluorescein isothiocyanate (FITC)- or Cy3-conjugated secondary antibodies (Jackson ImmunoResearch Laboratories, West Grove, PA). Slides were mounted with Vectashield with 4′6-diamidino-2-phenylindole (DAPI) (Vector Labs). beta-cell apoptosis for mouse sections or primary islets cultured on ECM dishes was analyzed by the terminal deoxynucleotidyl transferase-mediated dUTP nick-end labeling (TUNEL) technique according to the manufacturer's instructions (In Situ Cell Death Detection Kit, TMR red; Roche) and double stained for insulin. Fluorescence was analyzed using a Nikon MEA53200 (Nikon GmbH, Dusseldorf, Germany) microscope and images were acquired using NIS-Elements software (Nikon).

Morphometric analysis

For morphometric data, ten sections (spanning the width of the pancreas) per mouse were analyzed. Pancreatic tissue area and insulin-positive area were determined by computer-assisted measurements using a Nikon MEA53200 (Nikon GmbH, Dusseldorf, Germany) microscope and images were acquired using NIS-Elements software (Nikon). The number of islets (defined as insulin-positive aggregates at least 25 μm in diameter) was scored and used to calculate islet density (number of islets per square centimeter of tissue), mean islet size (the ratio of the total insulin-positive area to the total islet number on the sections). Mean percent beta-cell fraction per pancreas was calculated as the ratio of insulin-positive and whole pancreatic tissue area. Beta-cell mass was obtained by multiplying the beta cell fraction by the weight of the pancreas. Morphometric beta-cell and islet characterizations are results from analyses of at least 100 islets per mouse.

Western Blot analysis

At the end of the incubation periods, islets and INS-1E cells were washed in ice-cold PBS and lysed in lysis buffer containing 20 mM Tris acetate, 0.27 M sucrose, 1 mM EDTA, 1

mM EGTA, 50mM NaF, 1% Triton X-100, 5 mM sodium pyrophosphate and 10 mM β-glycerophosphate. Prior to use, the lysis buffer was supplemented with Protease- and Phosphatase-inhibitors (Pierce, Rockford, IL, USA). Protein concentrations were determined with the BCA protein assay (Pierce). Equivalent amounts of protein from each treatment group were run on a NuPAGE 4-12% Bis-Tris gel (Invitrogen) and electrically transferred onto PVDF membranes. After 1h blocking at room temperature using 5% milk (Cell Signaling), membranes were incubated overnight at 4°C with rabbit anti-MST1, rabbit anti-P-MST1, rabbit anti-Bim, rabbit anti-P-AKT (Ser437), rabbit anti-Bax, rabbit anti-Bcl-2, rabbit anti-Bcl-xL, rabbit anti-Bad, rabbit anti-phospho Bad, rabbit anti-PUMA, rabbit anti-Bak, rabbit anti-Mcl1, rabbit anti-pan-phopsho threonine, mouse monoclonal anti-pan-phospho threonine, rabbit anti-phospho GSK-3, rabbit anti-phospho FOXO1, mouse anti-Myc, rabbit anti-cleaved caspase-3, rabbit anti-cleaved caspase-9, rabbit anti-cytochrome *c*, rabbit anti-cytochrom oxidase (COX), rabbit anti-phospho JNK (Thr183/Tyr185), rabbit anti-phospho c-Jun (Ser63), rabbit anti-PARP, rabbit anti-tubulin, rabbit anti-GAPDH and rabbit anti-β-actin (all Cell Signaling Technology), rabbit anti-P-MST1, rabbit anti-GFP, mouse anti-NOXA and rabbit anti-PDX1 (Abcam), rabbit anti-P-H2B (Millipore) and rabbit anti-P-PDX1 (Thr11) (Abgent) antibodies, followed by horseradish-peroxidase-linked anti-rabbit or mouse IgG (Jackson). Membrane was developed using a chemiluminescence assay system (Pierce) and analyzed using DocIT®LS image acquisition 6.6a (UVP BioImaging Systems, Upland, CA, USA).

Immunoprecipitation

For immunoprecipitation, cells were washed with PBS and lysed in cold buffer containing 20 mM Tris-HCl (pH 7.5), 150 mM NaCl, 0.27 M sucrose, 1 mM EDTA, 1 mM EGTA, 50 mM NaF, 1% NP-40, 5 mM sodium pyrophosphate and 10 mM β-glycerophosphate supplemented with proteinase/phosphatase inhibitors for 30 min on ice. Lysates were centrifuged at 12,000 g for 15 min at 4°C prior to immunoprecipitation. Immunoprecipitations were carried out with incubating 0.5-1 mg of total lysate with rabbit anti-PDX1 (1:500), rabbit anti-MST1 (1:50), mouse anti-Myc (1:1000) and rabbit anti-GFP (1:1000) antibodies on a rotator at 4°C overnight. Immunocomplexes were then captured with Protein A Agarose Fast Flow (Millipore) by rotation at 4°C for 4 h. After five washes with cold lysis buffer, the immunoprecipitates were used for kinase assays or resuspended in sample buffer and separated by NuPAGE 4-12% Bis-Tris gels (Invitrogen).

In vitro kinase assay

Purified human active MST1 (Upstate Biotechnology) with or without GST tag was incubated with ^{32}P-ATP (2 μCi, Perkin Elmer Life Sciences), ATP (100 μM) and 1 mM dithiothreitol (DTT) in a kinase buffer containing 40 mM HEPES (pH 7.4), 20 mM MgCl2, 1mM EDTA and 1 μg of purified recombinant human PDX-1 (Abcam) or bacterially purified GST-PDX1 (WT and mutants) as substrates. After incubation at 30°C for 30 min, the reaction was stopped by adding loading buffer and proteins were separated on NuPAGE gels and phosphorylation levels visualized either by autoradiography or specific antibody for phospho-PDX1. The total PDX1 was detected with anti-PDX1 antibody.

In vivo kinase assay

HEK293 cells were transiently transfected with PDX1 and MST1 expression plasmids. Then, cell lysates were subjected to immunoprecipitation with anti-PDX1 antibody. The immunoprecipitates were separated by NuPAGE Bis-Tris gels and transferred to PVDF membranes and subsequently subjected to analyses of phosphorylation levels by pan phospho-threonine antibody, which binds to threonine-phosphorylated sites in a manner

largely independent of the surrounding amino-acid sequence or pan phospho-serine antibody which is recognizes serine-phosphorylated proteins.

In vivo ubiquitination

HEK293 cells were cultured in 10-cm cell culture dishes and transfected with HA-ubiquitin, PDX1 and MST1 expression plasmids for 48h. For ubiquitination in human islets, 5000 islets per condition were transfected with ubiquitin plasmid. After 24h, islets were infected with Ad-GFP or Ad-MST1 for 6h and kept for another 48h. HEK293 cells and islets were exposed to 20 μM MG-132 for the last 6h of the experiment. Lysates were immunoprecipitated with PDX1-specific antibody overnight at 4°C. Immunocomplexes were then captured with Protein A Agarose by rotation at 4°C for 4h. After extensive washing, immunoprecipitates were boiled in sample buffer and proteins subjected to western blotting with ubiquitin-specific antibody.

Protein degradation analysis

HEK293 cells were transfected with PDX1 alone, or together with MST1 expressing-plasmids. Human islets were infected with Ad-GFP (control) or Ad-MST1. At 48h after post-transfection/ infection, cells were treated with 50 μg/ml translation initiation inhibitor cycloheximde (CHX) to the medium at the times indicated and the lysates were subjected to western blotting.

RNA extraction and RT-PCR analysis

Total RNA was isolated from cultured human islets and INS-1E cells using TRIzol (Invitrogen), and RT-PCR performed as described previously [67]. For analysis, we used the Applied Biosystems StepOne Real-Time PCR system (Applied Biosystems, CA, USA) with TaqMan(R) Fast Universal PCR Master Mix for TaqMan assays (Applied Biosystems). TaqMan(R) Gene Expression Assays were used for pdx1 (Hs00426216_m1), SLC2A2 (Hs01096905_m1), GCK (Hs01564555_m1), insulin (Hs02741908_m1), PPIA (Hs99999904_m1), BCL2L11 (Hs01083836_m1) and tubulin (Hs00362387_m1) for human and PDX1 (Rn00755591_m1), SLC2A2 (Rn00563565_m1), GCK (Rn00688285_m1), INS1 (Rn02121433_g1), INS2 (Rn01774648_g1), PPIA (Rn00690933_m1) and tuba1a (Rn01532518_g1) for rat.

Luciferase reporter assay

The transcriptional activity of the PDX1 at promoter level was evaluated using rat Ins2-Luc renilla reporter gene HEK293 cells were transfected with Ins2-Luc renilla, pCMV-firefly, PDX1-WT or PDX1-T11A, alone or together with Myc-MST1 expressing plasmids for 48h. INS-1E cells transfected with Ins2-Luc renilla and pCMV-firefly plasmids and were infected with Ad-GFP or Ad-MST1 for 48h. Luciferase activity determined using the Renilla-Firefly Luciferase Dual Assay Kit according to the manufacturer's instructions (Pierce). pCMV-firefly was used as transfection control.

Adenovirus Infection

Isolated human islets and INS-1E cells were infected with adenovirus carrying e-GFP as a control (kindly provided by Dr. Allan E. Karlsen, Novo Nordisk A/S, Denmark) or MST1 (AdX-MST1, kindly provided by Dr. Sadoshima) at a multiplicity of infection (MOI) of 20 (for INS-1E) or 100 (for human islets) for 4h. Adenovirus was subsequently washed off with PBS and replaced by fresh medium with 10% FBS and GSIS or RNA and protein isolation performed after 48 or 72 h post-infection.

Europe PMC Funders Author Manuscripts

Purification of GST-PDX1 recombinant proteins

Expression and induction of recombinant GST proteins were performed as described previously [68]. Escherichia coli BL21 cells with various GST-fusion expression plasmids were cultured at 37°C and expression of recombinant proteins was induced by 0.1mM final concentration of Isopropyl-β-D-thio-galactoside (IPTG; sigma) for 2.5h. Cells were lysed using B-PER bacterial protein extraction reagent (Pierce) and purified using Glutathione Spin Columns (Pierce).

Cytochrome *c* release

Cytochrome c release was performed by digitonin-based subcellular fractionation technique [69]. Briefly, INS-1E cells were digitonin-permeabilized for 5min on ice after resuspension of the cell pellet in 200 μl of cytosolic extraction buffer (CEB: 250 mM sucrose, 70 mM KCl, 137 mM NaCl, 4.3 mM Na2HPO4, 1.4 mM KH2PO4 (pH 7.2), with 300 μg/ml digitonin (Sigma). Cells were then centrifuged at 1000g for 5min at 4°C. Supernatants (cytosolic fractions) were collected and pellets solubilized in the same volume of mitochondrial lysis buffer (MLB: 50 mM Tris, pH 7.4, 150 mM NaCl, 2 mM EDTA, 2 mM EGTA, 0.2% Triton X-100, 0.3% NP-40), followed by centrifugation at 10,000g for 10 min at 4 C. After centrifugation, supernatants, which are the heavy membrane fractions enriched for mitochondria as well as cytosolic fractions were subjected to western blot analysis.

Generation of stably expressed shRNAmir-MST1 INS1 cell line

To knock down MST1 expression in INS-1E cells, two different lentiviral shRNAmir targeting MST1 or control shRNAmir vectors (pGIPZ collection, Open Biosystems, Huntsville, AL) were transfected into INS-1E cells and stable clones were generated by selection with puromycin (1 to 2.5 μg/ml). Positive clonal cell lines were identified by immunoblotting using antibody directed against MST1. After selection, INS-1E lines were maintained in culture medium containing 1.5 μg/ml puromycin.

Statistical analysis

Samples were evaluated in a randomized manner by five investigators (A.A., V.K., S.K., T.Y., Z.A.) who were blinded to the treatment conditions. Data are presented as means +/− SE. Mean differences were tested by Student's *t*- tests. To account for multiplicity in the treated cells in vitro and mice in vivo, a Bonferroni correction used.

Supplementary Material

Refer to Web version on PubMed Central for supplementary material.

Acknowledgments

This work was supported by the JDRF, the German Research Foundation (DFG, Emmy Noether Programm MA4172/1-1), the European Research Council (ERC), the Diabetes Competence Network (KKNDm) supported by the German Federal Ministry of Science (BMBF) and by University of Bremen Research Funds. We thank Jennifer Bergemann for excellent technical assistance, Gitanjali Dharmadhikari and Madhura Panse for help with the analyses (all University of Bremen), Guy Rutter (Imperial College London) and Desiree Schumann (Boehringer Ingelheim) for the critical discussion. Human islets were provided through the JDRF award 31-2008-413 (ECIT Islet for Basic Research program) and by the integrated islet distribution program (IIDP). Human pancreatic sections were provided from the National Disease Research Interchange (NDRI), supported by the NIH. MST1 and dnMST1 plasmids and adenoviruses were kindly provided by Junichi Sadoshima and Yasuhiro Maejima (Rutgers New Jersey Medical School), PDX-1WT plasmids from Reinhard Walther (University of Greifswald), INS-1E cells from Claes Wollheim (Lund and Geneva Universities), Rip-Cre mice from Pedro Herrera (University of Geneva) and Ahmed Mansouri (Max Planck Institute for Biophysical Chemistry).

References

1. Kurrer MO, Pakala SV, Hanson HL, Katz JD. Beta cell apoptosis in T cell-mediated autoimmune diabetes. Proc.Natl.Acad.Sci.U.S.A. 1997; 94:213–218. [PubMed: 8990188]
2. Mathis D, Vence L, Benoist C. beta-Cell death during progression to diabetes. Nature. 2001; 414:792–798. [PubMed: 11742411]
3. Butler AE, et al. Beta-cell deficit and increased beta-cell apoptosis in humans with type 2 diabetes. Diabetes. 2003; 52:102–110. [PubMed: 12502499]
4. Rhodes CJ. Type 2 diabetes-a matter of beta-cell life and death? Science. 2005; 307:380–384. [PubMed: 15662003]
5. Donath MY, Storling J, Maedler K, Mandrup-Poulsen T. Inflammatory mediators and islet beta-cell failure: a link between type 1 and type 2 diabetes. J.Mol.Med. 2003; 81:455–470. [PubMed: 12879149]
6. The Diabetes Control and Complications Trial Research Group. Effect of intensive therapy on residual beta-cell function in patients with type 1 diabetes in the diabetes control and complications trial. A randomized, controlled trial. Ann Intern Med. 1998; 128:517–523. [PubMed: 9518395]
7. Lenzen S, Drinkgern J, Tiedge M. Low antioxidant enzyme gene expression in pancreatic islets compared with various other mouse tissues. Free Radic Biol Med. 1996; 20:463–466. [PubMed: 8720919]
8. Ling P, Lu TJ, Yuan CJ, Lai MD. Biosignaling of mammalian Ste20-related kinases. Cell Signal. 2008; 20:1237–1247. [PubMed: 18255267]
9. Avruch J, et al. Protein kinases of the Hippo pathway: regulation and substrates. Semin Cell Dev Biol. 2012; 23:770–784. [PubMed: 22898666]
10. Lee KK, et al. Proteolytic activation of MST/Krs, STE20-related protein kinase, by caspase during apoptosis. Oncogene. 1998; 16:3029–3037. [PubMed: 9662336]
11. Kakeya H, Onose R, Osada H. Caspase-mediated activation of a 36-kDa myelin basic protein kinase during anticancer drug-induced apoptosis. Cancer Res. 1998; 58:4888–4894. [PubMed: 9809995]
12. Bi W, et al. c-Jun N-terminal Kinase Enhances MST1-mediated Pro-apoptotic Signaling through Phosphorylation at Serine 82. J Biol Chem. 2010; 285:6259–6264. [PubMed: 20028971]
13. Cheung WL, et al. Apoptotic phosphorylation of histone H2B is mediated by mammalian sterile twenty kinase. Cell. 2003; 113:507–517. [PubMed: 12757711]
14. Jonsson J, Carlsson L, Edlund T, Edlund H. Insulin-promoter-factor 1 is required for pancreas development in mice. Nature. 1994; 371:606–609. [PubMed: 7935793]
15. Stoffers DA, Zinkin NT, Stanojevic V, Clarke WL, Habener JF. Pancreatic agenesis attributable to a single nucleotide deletion in the human IPF1 gene coding sequence. Nat Genet. 1997; 15:106–110. [PubMed: 8988180]
16. Johnson JD, et al. Increased islet apoptosis in Pdx1+/− mice. J.Clin.Invest. 2003; 111:1147–1160. [PubMed: 12697734]
17. Stoffers DA, Ferrer J, Clarke WL, Habener JF. Early-onset type-II diabetes mellitus (MODY4) linked to IPF1. Nat Genet. 1997; 17:138–139. [PubMed: 9326926]
18. Brissova M, et al. Reduction in pancreatic transcription factor PDX-1 impairs glucose-stimulated insulin secretion. J Biol Chem. 2002; 277:11225–11232. [PubMed: 11781323]
19. Ardestani A, et al. Neutralizing interleukin-1beta (IL-1beta) induces beta-cell survival by maintaining PDX1 protein nuclear localization. J Biol Chem. 2011; 286:17144–17155. [PubMed: 21393239]
20. Lee KK, Ohyama T, Yajima N, Tsubuki S, Yonehara S. MST, a physiological caspase substrate, highly sensitizes apoptosis both upstream and downstream of caspase activation. J Biol Chem. 2001; 276:19276–19285. [PubMed: 11278283]
21. Tuttle RL, et al. Regulation of pancreatic beta-cell growth and survival by the serine/threonine protein kinase Akt1/PKBalpha. Nat Med. 2001; 7:1133–1137. [PubMed: 11590437]
22. Bernal-Mizrachi E, Wen W, Stahlhut S, Welling CM, Permutt MA. Islet beta cell expression of constitutively active Akt1/PKB alpha induces striking hypertrophy, hyperplasia, and hyperinsulinemia. J Clin Invest. 2001; 108:1631–1638. [PubMed: 11733558]

23. Yuan Z, et al. Phosphoinositide 3-kinase/Akt inhibits MST1-mediated pro-apoptotic signaling through phosphorylation of threonine 120. J Biol Chem. 2010; 285:3815–3824. [PubMed: 19940129]
24. Cinar B, et al. The pro-apoptotic kinase Mst1 and its caspase cleavage products are direct inhibitors of Akt1. EMBO J. 2007; 26:4523–4534. [PubMed: 17932490]
25. Trumper K, et al. Integrative mitogenic role of protein kinase B/Akt in beta-cells. Ann N Y Acad Sci. 2000; 921:242–250. [PubMed: 11193829]
26. Matallanas D, et al. RASSF1A elicits apoptosis through an MST2 pathway directing proapoptotic transcription by the p73 tumor suppressor protein. Mol Cell. 2007; 27:962–975. [PubMed: 17889669]
27. Valis K, et al. Hippo/Mst1 stimulates transcription of the proapoptotic mediator NOXA in a FoxO1-dependent manner. Cancer Res. 2011; 71:946–954. [PubMed: 21245099]
28. Grunnet LG, et al. Proinflammatory cytokines activate the intrinsic apoptotic pathway in beta-cells. Diabetes. 2009; 58:1807–1815. [PubMed: 19470609]
29. Opferman JT, Korsmeyer SJ. Apoptosis in the development and maintenance of the immune system. Nat Immunol. 2003; 4:410–415. [PubMed: 12719730]
30. Yamamoto S, et al. Activation of Mst1 causes dilated cardiomyopathy by stimulating apoptosis without compensatory ventricular myocyte hypertrophy. J Clin Invest. 2003; 111:1463–1474. [PubMed: 12750396]
31. Lei K, Davis RJ. JNK phosphorylation of Bim-related members of the Bcl2 family induces Bax-dependent apoptosis. Proc Natl Acad Sci U S A. 2003; 100:2432–2437. [PubMed: 12591950]
32. Rahmani M, et al. The BH3-only protein Bim plays a critical role in leukemia cell death triggered by concomitant inhibition of the PI3K/Akt and MEK/ERK1/2 pathways. Blood. 2009; 114:4507–4516. [PubMed: 19773546]
33. Humphrey RK, Yu SM, Flores LE, Jhala US. Glucose regulates steady-state levels of PDX1 via the reciprocal actions of GSK3 and AKT kinases. J Biol Chem. 2010; 285:3406–3416. [PubMed: 19833727]
34. Kawamori D, et al. The forkhead transcription factor Foxo1 bridges the JNK pathway and the transcription factor PDX-1 through its intracellular translocation. J Biol Chem. 2006; 281:1091–1098. [PubMed: 16282329]
35. McCulloch LJ, et al. GLUT2 (SLC2A2) is not the principal glucose transporter in human pancreatic beta cells: implications for understanding genetic association signals at this locus. Mol Genet Metab. 2011; 104:648–653. [PubMed: 21920790]
36. Claiborn KC, et al. Pcif1 modulates Pdx1 protein stability and pancreatic beta cell function and survival in mice. J Clin Invest. 2010; 120:3713–3721. [PubMed: 20811152]
37. Miller ML, et al. Linear motif atlas for phosphorylation-dependent signaling. Sci Signal. 2008; 1:ra2. [PubMed: 18765831]
38. Frogne T, Sylvestersen KB, Kubicek S, Nielsen ML, Hecksher-Sorensen J. Pdx1 is post-translationally modified in vivo and serine 61 is the principal site of phosphorylation. PLoS One. 2012; 7:e35233. [PubMed: 22509401]
39. Dunning BE, Gerich JE. The role of alpha-cell dysregulation in fasting and postprandial hyperglycemia in type 2 diabetes and therapeutic implications. Endocr Rev. 2007; 28:253–283. [PubMed: 17409288]
40. Li Z, Karlsson FA, Sandler S. Islet loss and alpha cell expansion in type 1 diabetes induced by multiple low-dose streptozotocin administration in mice. J Endocrinol. 2000; 165:93–99. [PubMed: 10750039]
41. Lin Y, Khokhlatchev A, Figeys D, Avruch J. Death-associated protein 4 binds MST1 and augments MST1-induced apoptosis. J Biol Chem. 2002; 277:47991–48001. [PubMed: 12384512]
42. Del Re DP, et al. Proapoptotic Rassf1A/Mst1 signaling in cardiac fibroblasts is protective against pressure overload in mice. J Clin Invest. 2010; 120:3555–3567. [PubMed: 20890045]
43. Graves JD, Draves KE, Gotoh Y, Krebs EG, Clark EA. Both phosphorylation and caspase-mediated cleavage contribute to regulation of the Ste20-like protein kinase Mst1 during CD95/Fas-induced apoptosis. J Biol Chem. 2001; 276:14909–14915. [PubMed: 11278782]

44. Graves JD, et al. Caspase-mediated activation and induction of apoptosis by the mammalian Ste20-like kinase Mst1. EMBO J. 1998; 17:2224–2234. [PubMed: 9545236]
45. Song H, et al. Mammalian Mst1 and Mst2 kinases play essential roles in organ size control and tumor suppression. Proc Natl Acad Sci U S A. 2010; 107:1431–1436. [PubMed: 20080598]
46. Zhou D, et al. Mst1 and Mst2 maintain hepatocyte quiescence and suppress hepatocellular carcinoma development through inactivation of the Yap1 oncogene. Cancer Cell. 2009; 16:425–438. [PubMed: 19878874]
47. Yun HJ, et al. Daxx mediates activation-induced cell death in microglia by triggering MST1 signalling. EMBO J. 2011; 30:2465–2476. [PubMed: 21572393]
48. Odashima M, et al. Inhibition of endogenous Mst1 prevents apoptosis and cardiac dysfunction without affecting cardiac hypertrophy after myocardial infarction. Circ Res. 2007; 100:1344–1352. [PubMed: 17395874]
49. Assmann A, Ueki K, Winnay JN, Kadowaki T, Kulkarni RN. Glucose effects on beta-cell growth and survival require activation of insulin receptors and insulin receptor substrate 2. Mol Cell Biol. 2009; 29:3219–3228. [PubMed: 19273608]
50. Ahlgren U, Jonsson J, Jonsson L, Simu K, Edlund H. beta-cell-specific inactivation of the mouse Ipf1/Pdx1 gene results in loss of the beta-cell phenotype and maturity onset diabetes. Genes Dev. 1998; 12:1763–1768. [PubMed: 9637677]
51. Lebrun P, Montminy MR, Van Obberghen E. Regulation of the pancreatic duodenal homeobox-1 protein by DNA-dependent protein kinase. J Biol Chem. 2005; 280:38203–38210. [PubMed: 16166097]
52. Costes S, et al. beta-cell dysfunctional ERAD/ubiquitin/proteasome system in type 2 diabetes mediated by islet amyloid polypeptide-induced UCH-L1 deficiency. Diabetes. 2011; 60:227–238. [PubMed: 20980462]
53. Butler PC, Meier JJ, Butler AE, Bhushan A. The replication of beta cells in normal physiology, in disease and for therapy. Nat Clin Pract Endocrinol Metab. 2007; 3:758–768. [PubMed: 17955017]
54. Choi J, et al. Mst1-FoxO signaling protects Naive T lymphocytes from cellular oxidative stress in mice. PLoS One. 2009; 4:e8011. [PubMed: 19956688]
55. Dong Y, et al. A cell-intrinsic role for Mst1 in regulating thymocyte egress. J Immunol. 2009; 183:3865–3872. [PubMed: 19692642]
56. Ueda Y, et al. Mst1 regulates integrin-dependent thymocyte trafficking and antigen recognition in the thymus. Nat Commun. 2012; 3:1098. [PubMed: 23033074]
57. Soltani N, et al. GABA exerts protective and regenerative effects on islet beta cells and reverses diabetes. Proc Natl Acad Sci U S A. 2011; 108:11692–11697. [PubMed: 21709230]
58. Sauter NS, Schulthess FT, Galasso R, Castellani LW, Maedler K. The antiinflammatory cytokine interleukin-1 receptor antagonist protects from high-fat diet-induced hyperglycemia. Endocrinology. 2008; 149:2208–2218. [PubMed: 18239070]
59. Carew RM, et al. Deletion of Irs2 causes reduced kidney size in mice: role for inhibition of GSK3beta? BMC Dev Biol. 2010; 10:73. [PubMed: 20604929]
60. Kawano Y, et al. Loss of Pdk1-Foxo1 signaling in myeloid cells predisposes to adipose tissue inflammation and insulin resistance. Diabetes. 2012; 61:1935–1948. [PubMed: 22586579]
61. Schulthess FT, et al. CXCL10 impairs beta cell function and viability in diabetes through TLR4 signaling. Cell Metab. 2009; 9:125–139. [PubMed: 19187771]
62. Maedler K, et al. Distinct effects of saturated and monounsaturated fatty acids on beta-cell turnover and function. Diabetes. 2001; 50:69–76. [PubMed: 11147797]
63. Herrera PL. Adult insulin- and glucagon-producing cells differentiate from two independent cell lineages. Development. 2000; 127:2317–2322. [PubMed: 10804174]
64. Surwit RS, Kuhn CM, Cochrane C, McCubbin JA, Feinglos MN. Diet-induced type II diabetes in C57BL/6J mice. Diabetes. 1988; 37:1163–1167. [PubMed: 3044882]
65. Kang HC, Bae YH. Transfection of rat pancreatic islet tissue by polymeric gene vectors. Diabetes Technol Ther. 2009; 11:443–449. [PubMed: 19580358]
66. Shu L, et al. Transcription factor 7-like 2 regulates beta-cell survival and function in human pancreatic islets. Diabetes. 2008; 57:645–653. [PubMed: 18071026]

67. Shu L, et al. TCF7L2 promotes beta cell regeneration in human and mouse pancreas. Diabetologia. 2012

68. Tolia NH, Joshua-Tor L. Strategies for protein coexpression in Escherichia coli. Nat Methods. 2006; 3:55–64. [PubMed: 16369554]

69. Arnoult D. Apoptosis-associated mitochondrial outer membrane permeabilization assays. Methods. 2008; 44:229–234. [PubMed: 18314053]

Europe PMC Funders Author Manuscripts

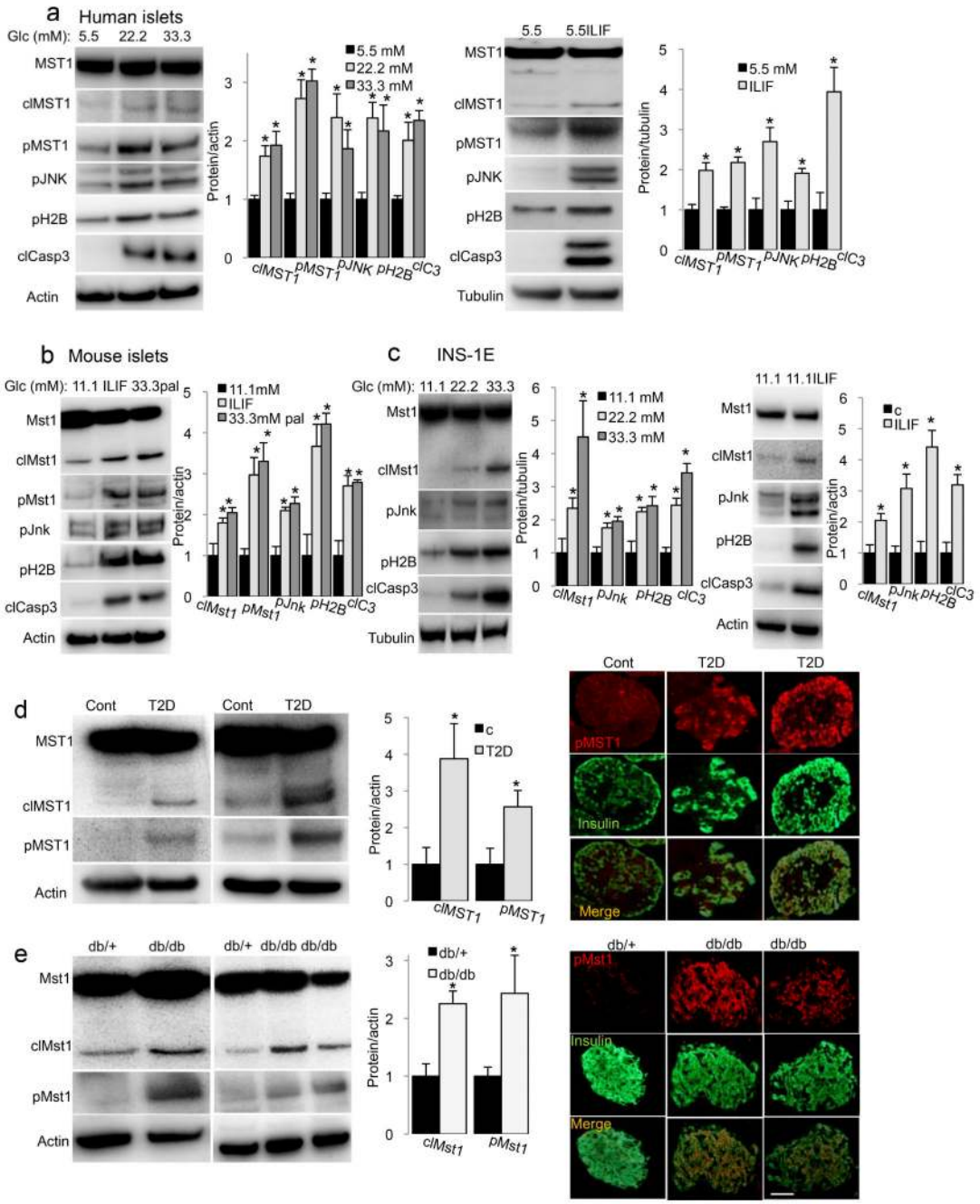

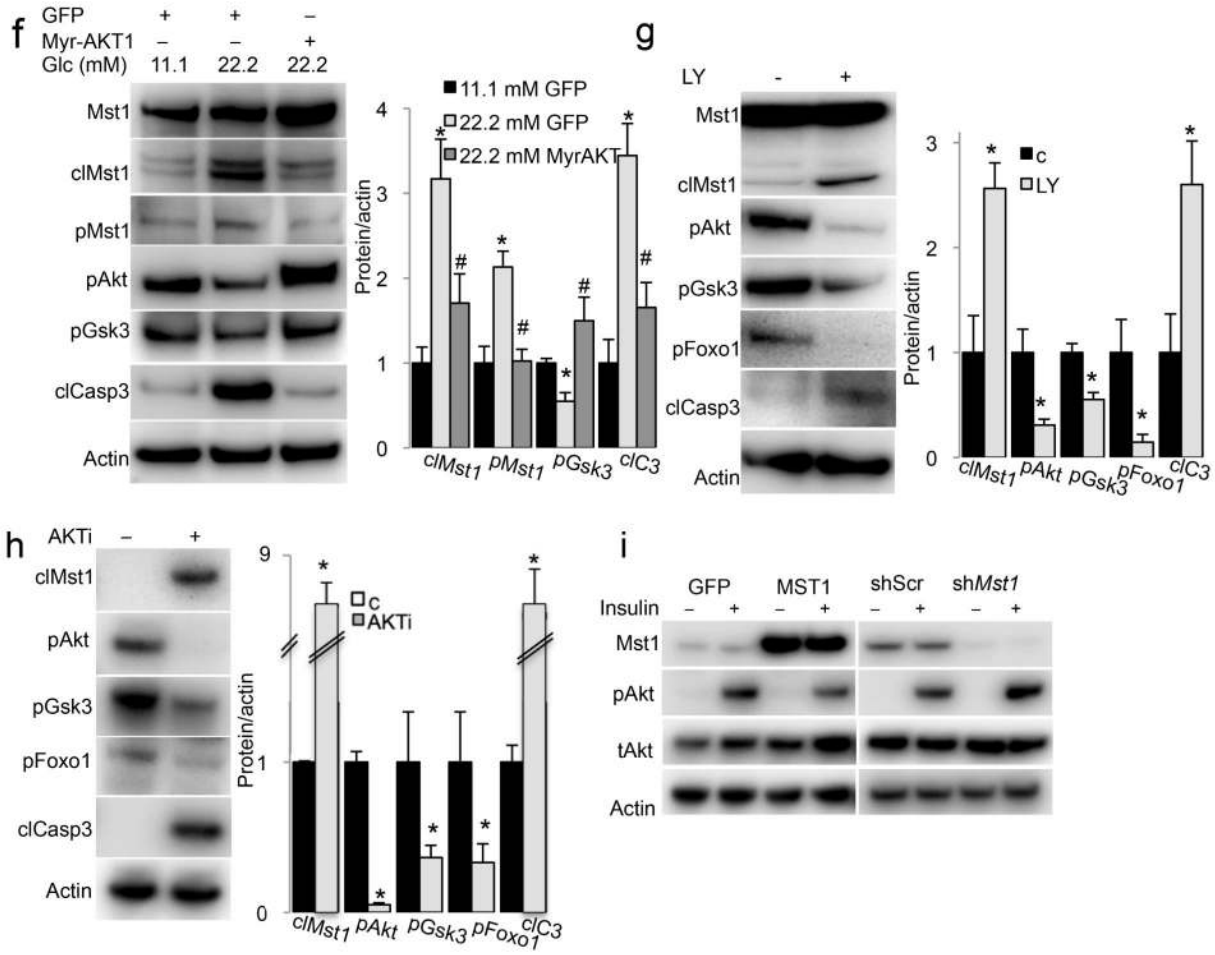

Figure 1. MST1 is activated in diabetes

(a-c) Activated MST1 (cleaved and phosphorylated) in human **(a)** and mouse **(b)** islets and INS1-E cells **(c)** exposed to diabetogenic conditions (22.2-33.3 mM glucose or the mixture of 33.3 mM glucose and 0.5 mM palmitate (33.3Palm) or IL-1β/IFNγ (IL/IF) for 72h. MST1, pMST1, pJNK, pH2B and caspase-3 cleavage were analyzed by western blotting, right panels show densitometry analysis from at least 3 independent experiments normalized to actin or tubulin. **(d,e)** Activated MST1 in diabetic islets. **(d)** Human isolated islets from non-diabetic controls (n=7) and subjects with T2D (n=4), all with documented fasting plasma glucose >150 mg/dl and **(e)** from 10-week old diabetic *db/db* (n=5) and their heterozygous *db*/+ littermates (n=5). MST1 and pMST1 were analyzed by western blotting, right panels show densitometry analysis normalized to actin. Right panels show double immunostaining for pMST1 in red and insulin in green in sections from human isolated islets from non-diabetic controls and subjects with T2D and from 6-week old diabetic db/db mice (representative analyses from 10 pancreases from subjects with T2D and >10 controls and from 7 *db/db* and 7 *db*/+ controls are shown, bar is 100 μM). **(f)** INS-1E cells transfected with GFP control or Myr-AKT1 expression-plasmids and exposed to 22.2 mM glucose for 72h. **(g,h)** PI3K/AKT was inhibited in INS-1E cells by exposure to **(g)** PI3K inhibitor, LY294002 (10 μM for 8h) or **(h)** AKT inhibitor Triciribine (10 μM for 6h). **(i)** INS-1E infected with Ad-GFP or Ad-MST1 or transfected with shMST1 or shScr control expression plasmids for 48h, serum-starved for 12h and then stimulated with insulin. Mst1, pMst1, pAkt, tAkt, pGsk3, pFoxo1 and caspase-3 cleavage were analyzed by western

Europe PMC Funders Author Manuscripts

blotting. Right panels show densitometry analysis from at least 3 independent experiments normalized to actin. All western blots show representative results from at least 3 independent experiments from 3 different donors or mice. Tubulin/Actin was used as loading control. Results shown are means ±SE. *p<0.05 compared to untreated or nondiabetic control. #p<0.05 Myr-AKT1 compared to GFP at 22.2 mM glucose.

Europe PMC Funders Author Manuscripts

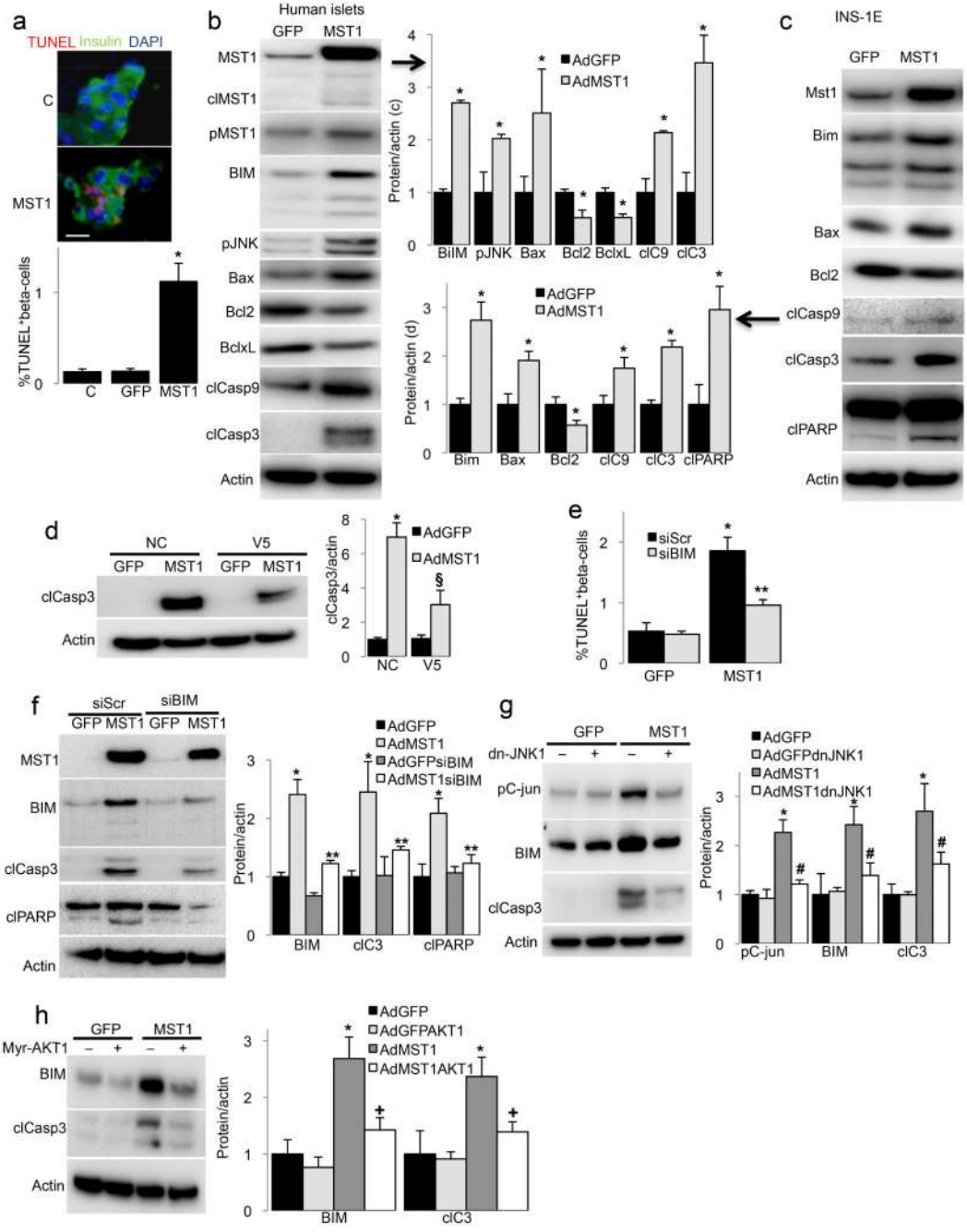

Figure 2. MST1 induces beta-cell death

(a-d) MST1 overexpression in human islets **(a,b)** and INS-1E cells **(c)** for 48h. Beta-cell apoptosis was analyzed by triple staining for DAPI (blue), TUNEL (red) and insulin (green; **a**). An average number of 18501 insulin-positive beta-cells were counted in 3 independent experiments from 3 different donors. **(b,c)** Efficient adenovirus-mediated up-regulation of MST1 and profiling expression levels of proteins of the mitochondrial death pathway. BIM, BAX, caspase-9 cleavage, BCL-2 and BCL-xL together with JNK activation and caspase-3 and PARP cleavage were analyzed by western blotting. **(d)** Exposure of Ad-GFP- or Ad-MST1-infected human islets to Bax-inhibitory peptide V5 or negative control (NC) peptide

for 36h. Caspase-3 cleavage was analyzed by western blotting. **(e,f)** Human islets transfected with BIM siRNA or control siScr were infected with Ad-GFP or Ad-MST1 for 48h. **(e)** Beta-cell apoptosis analyzed by double staining of TUNEL and insulin. An average number of 10378 insulin-positive beta-cells were counted in 3 independent experiments from 3 different donors. **(f)** MST1, BIM, caspase-3 and PARP cleavage were analyzed by western blotting. **(g)** Human islets transfected with GFP or dnJNK1 expressing-plasmids and infected with Ad-GFP or Ad-MST1 for 48h. PC-Jun, Bim and caspase-3 cleavage were analyzed by western blotting. **(h)** Human islets transfected with GFP or Myr-AKT1 expressing-plasmids and infected with Ad-GFP or Ad-MST1 for 48h. BIM and caspase-3 cleavage were analyzed by western blotting. Right **(b,d,f,g,h)/** left **(c)** panels show densitometry analysis from at least 3 independent experiments normalized to actin. All western blots show representative results from at least 3 independent experiments from 3 different donors (human islets). Actin was used as loading control. Results shown are means ±SE. *p<0.05 MST-OE compared to GFP control, §p<0.05 V5-MST1 compared to MST1, **p<0.05 siBim-MST1 compared to siScr-MST1, #p<0.05 dnJNK-MST1 compared to MST1, +p<0.05 AKT1-MST1 compared to MST1.

Europe PMC Funders Author Manuscripts

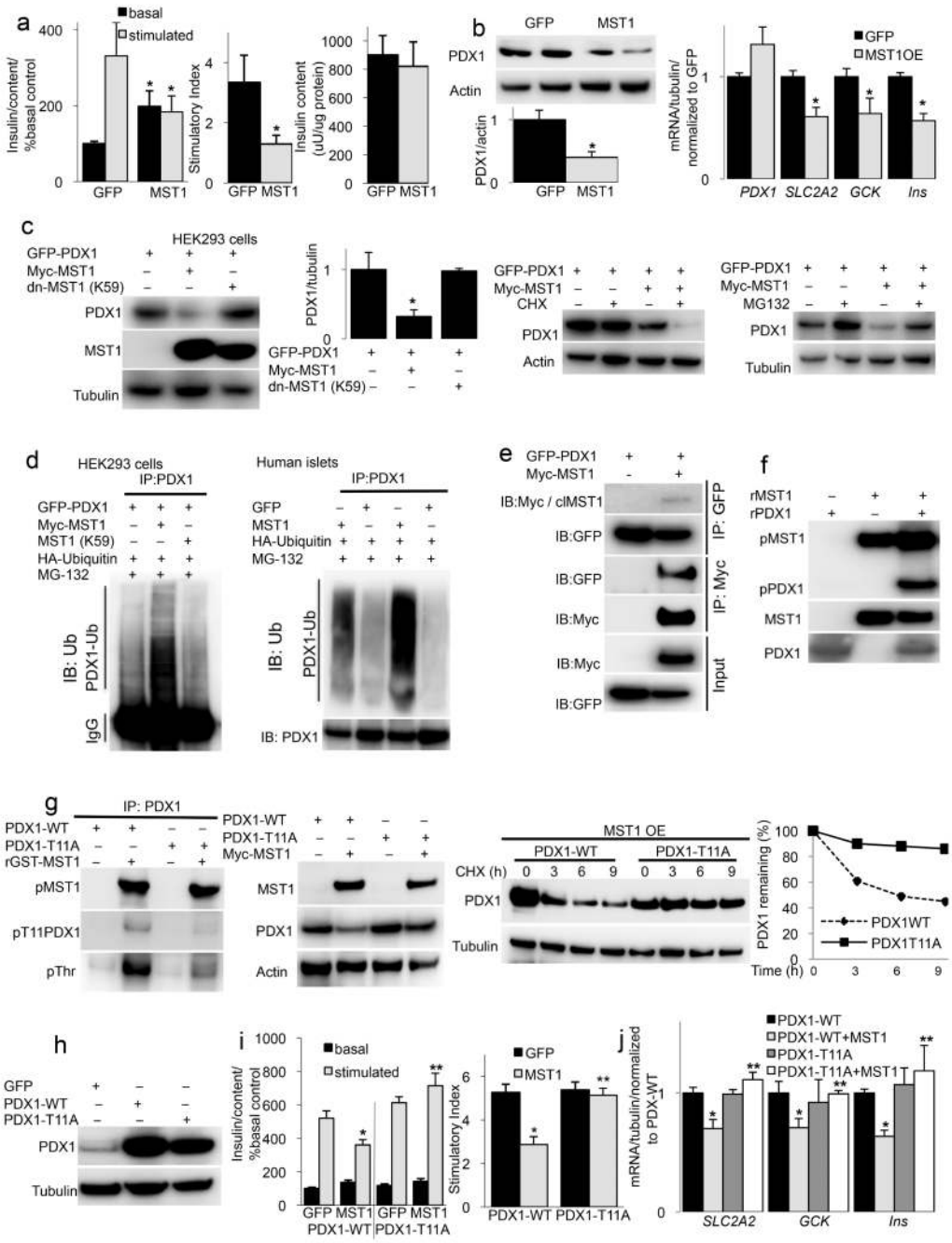

Figure 3. MST1 impairs beta-cell function by destabilizing PDX1

(a,b) Adenovirus-mediated GFP or MST1 overexpression in human islets for 96h. **(a)** Insulin secretion during 1h-incubation with 2.8 mM (basal) and 16.7 mM glucose (stimulated), normalized to insulin content and basal secretion at GFP control. The insulin stimulatory index denotes the ratio of secreted insulin during 1h-incubation with 16.7 mM and 2.8 mM glucose, respectively and insulin content analyzed after GSIS and normalized to whole islet protein. **(b)** MST1 and PDX1 immunoreactivity were analyzed by Western blotting. Lower panel shows densitometry analysis from at least 3 independent experiments normalized to actin. Right panel shows PDX1 target genes including *SLC2A2, GCK* and

Insulin analyzed by RT-PCR. **(c-d)** HEK293 cells were transfected with plasmids encoding Myc-MST1 and GFP-PDX1. **(c)** A kinase-dead MST1 (dn-MST1: K59R) was co-transfected with GFP-PDX1 (left panel). At 48 h after transfection, HEK293 cells were treated with cycloheximide (CHX) for 8h (middle panel). At 36h after transfection, HEK293 cells were treated with the proteasome inhibitor MG-132 for 6h (right panel). PDX1 and MST1 were analyzed by western blotting. **(d)** *In vivo* ubiquitination assay in HEK293 cells transfected with GFP-PDX1 and HA-ubiquitin, alone or together with Myc-MST1 or MST1-K59 expression plasmids for 48h (left) and human islets transfected with HA-ubiquitin and infected with Ad-GFP or Ad-MST1 for 48h (right; 2 different donors). MG-132 was added during the last 6h of the experiment. Cell lysates were immunoprecipitated with an anti-PDX1 antibody followed by immunoblotting with ubiquitin antibody to detect ubiquitinated PDX1. **(e)** HEK293 cells were transfected with GFP-PDX1 alone or together with Myc-MST1 for 48h. Reciprocal co-immunoprecipitations performed using anti-GFP and anti-Myc antibodies and western blot analysis performed with precipitates and input fraction using anti-Myc and anti-GFP antibodies, respectively. **(f)** *In vitro* kinase assay was performed by incubating recombinant MST1 and PDX1 proteins and analyzed by NuPAGE followed by western blotting using pan-phospho-threonine specific, PDX1 and MST1 antibodies. **(g)** Lysates of HEK293 cells transfected with PDX1-WT or PDX1-T11A expression-plasmids were immunoprecipitated with PDX1 antibody and subjected to an *in vitro* kinase assay using recombinant MST1. Phosphorylation reactions were analyzed by Western blotting using p-T11-PDX1 specific and pan-phospho threonine antibodies (left panel). HEK293 cells were transfected with PDX1-WT or PDX1-T11A alone or together with MST1 expression-plasmids for 48h. MST1 and PDX1 were analyzed by western blotting (middle panel). PDX-1-WT or PDX1-T11A co-transfected with MST1 in HEK293 cells for 36h and treated with CHX, western blot analysis for PDX1 and densitometry analysis of bands (right panel). **(h)** Human islets transfected with GFP, PDX1-WT or PDX1-T11A expression-plasmids and western blot analysis for PDX1. **(i,j)** human islets were infected with Ad-GFP or Ad-MST1 for 72h. **(i)** Insulin secretion during 1h-incubation with 2.8 mM (basal) and 16.7 mM glucose (stimulated), normalized to insulin content and basal secretion at control. The insulin stimulatory index denotes the ratio of secreted insulin during 1h-incubation with 16.7 mM and 2.8 mM glucose, respectively. **(j)** PDX1 target genes in human islets analyzed by RT-PCR and levels normalized to tubulin and shown as change from PDX1-WT transfected islets. All western blots show representative results from at least 3 independent experiments from 3 different donors (human islets). Tubulin/Actin was used as loading control. RT-PCR **(b,j)** and GSIS **(a,i)** show pooled results from 3 independent experiments from 3 different donors. Results shown are means ±SE. *$p<0.05$ MST-OE compared to control, **$p<0.05$ PDX-1T11A-MST1 compared to PDX-1WT-MST1.

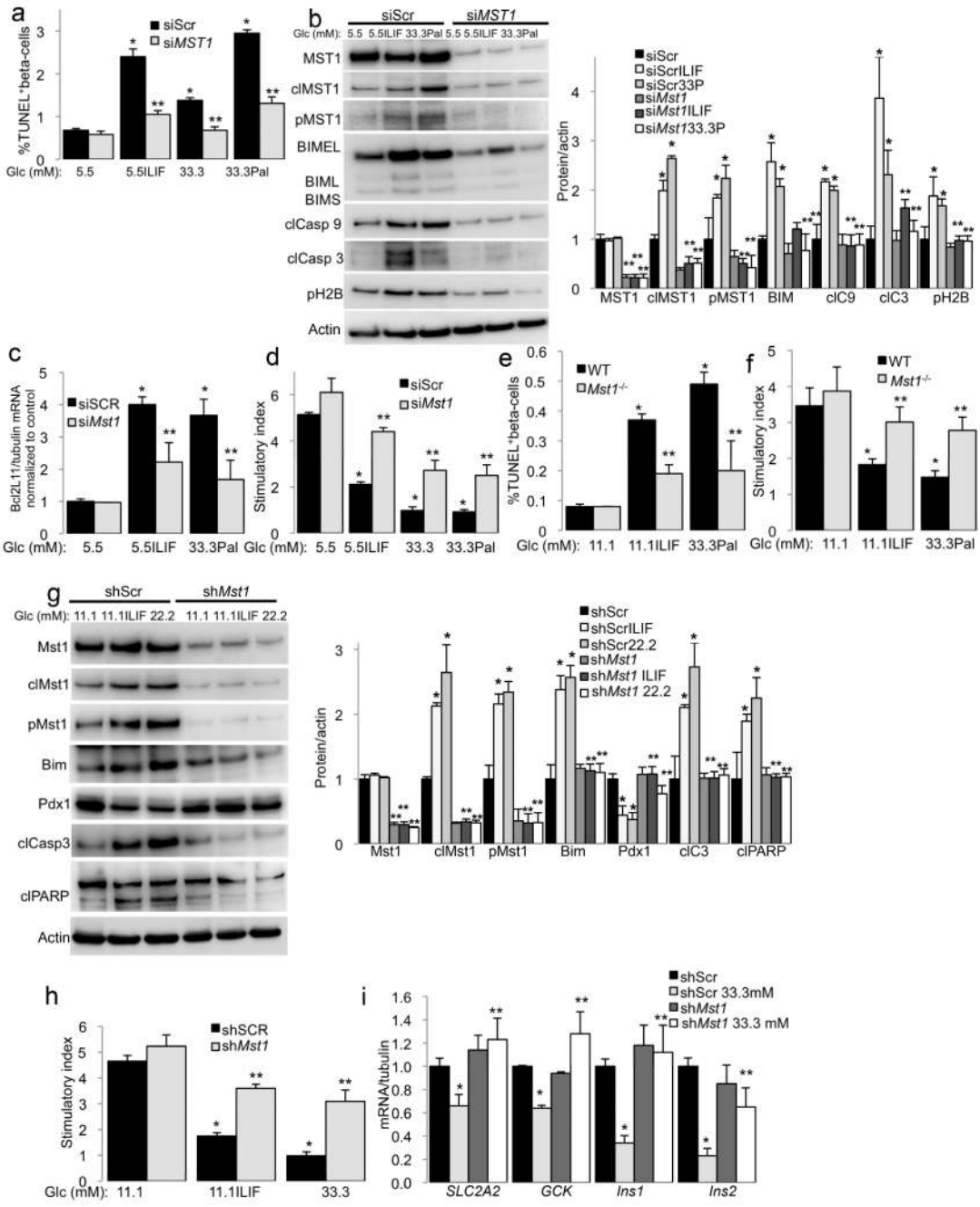

Figure 4. MST1 deficiency improves beta-cell survival and function

(a-d) Human islets transfected with MST1 siRNA or control siScr and treated with the cytokines mixture IL/IF, 33.3 mM glucose or the mixture of 33.3 mM glucose and 0.5 mM palmitate (33.3Pal) for 72h. **(a)** Beta-cell apoptosis analyzed by double staining of TUNEL and insulin. An average number of 11390 insulin-positive beta-cells were counted for each treatment condition in 3 independent experiments from 3 different donors. **(b)** Western blotting confirmed successful (~80%) MST1 depletion in human islets. MST1, pMST1, BIM, pH2B, caspase-9 and caspase-3 cleavage analyzes by western blotting. Right panel shows densitometry analysis from at least 3 independent experiments normalized to actin.

Europe PMC Funders Author Manuscripts

Europe PMC Funders Author Manuscripts

(c) RT-PCR for *BCL2L11* performed in human islets and levels normalized to tubulin shown as change from siScr control transfected islets. **(d)** Insulin stimulatory index denotes the ratio of secreted insulin during 1h-incubation with 16.7 mM and 1h-incubation with 2.8 mM glucose. **(e,f)** Islets were isolated from *Mst1*$^{-/-}$ mice and their WT littermates and exposed to the cytokines mixture IL/IF or the mixture of 33.3 mM glucose and 0.5 mM palmitate (33.3Pal) for 72 hours. **(e)** beta-cell apoptosis analyzed by double staining for TUNEL and insulin. An average number of 24180 insulin-positive beta-cells were counted for each treatment condition in 3 independent experiments. **(f)** Insulin stimulatory index denotes the ratio of secreted insulin during 1h-incubation with 16.7 mM and 1h-incubation with 2.8 mM glucose. **(g-i)** Stable INS-1E clones were generated by transfection of vectors for shMst1 and shScr control and treated with the cytokines mixture IL/IF or 22.2 or 33.3 mM glucose for 72h. **(g)** Mst1, Bim, Pdx1, caspase-3 and PARP cleavage were analyzed by western blotting. Right panel shows densitometry analysis from at least 3 independent experiments normalized to actin. **(h)** Insulin stimulatory index. **(i)** PDX1 target genes in shMst1 and shScr control INS-1E cells normalized to tubulin and shown as change from shScr control INS1-E clones. Western blots **(b,g)** show representative results from 3 independent experiments from 3 different donors (human islets). Actin was used as loading control. TUNEL data **(a,e),** GSIS **(d,f,h)** or RT-PCR **(c,i)** show pooled results from 3 independent experiments. Results shown are means ±SE. *p<0.05 compared to siScr **(a,b,c,d),** WT **(e,f)** or shScr untreated controls **(g,h,i)**, **p<0.05 compared to siScr **(a,b,c,d),** WT **(e,f)** or shScr **(g,h,i)** at the same treatment conditions.

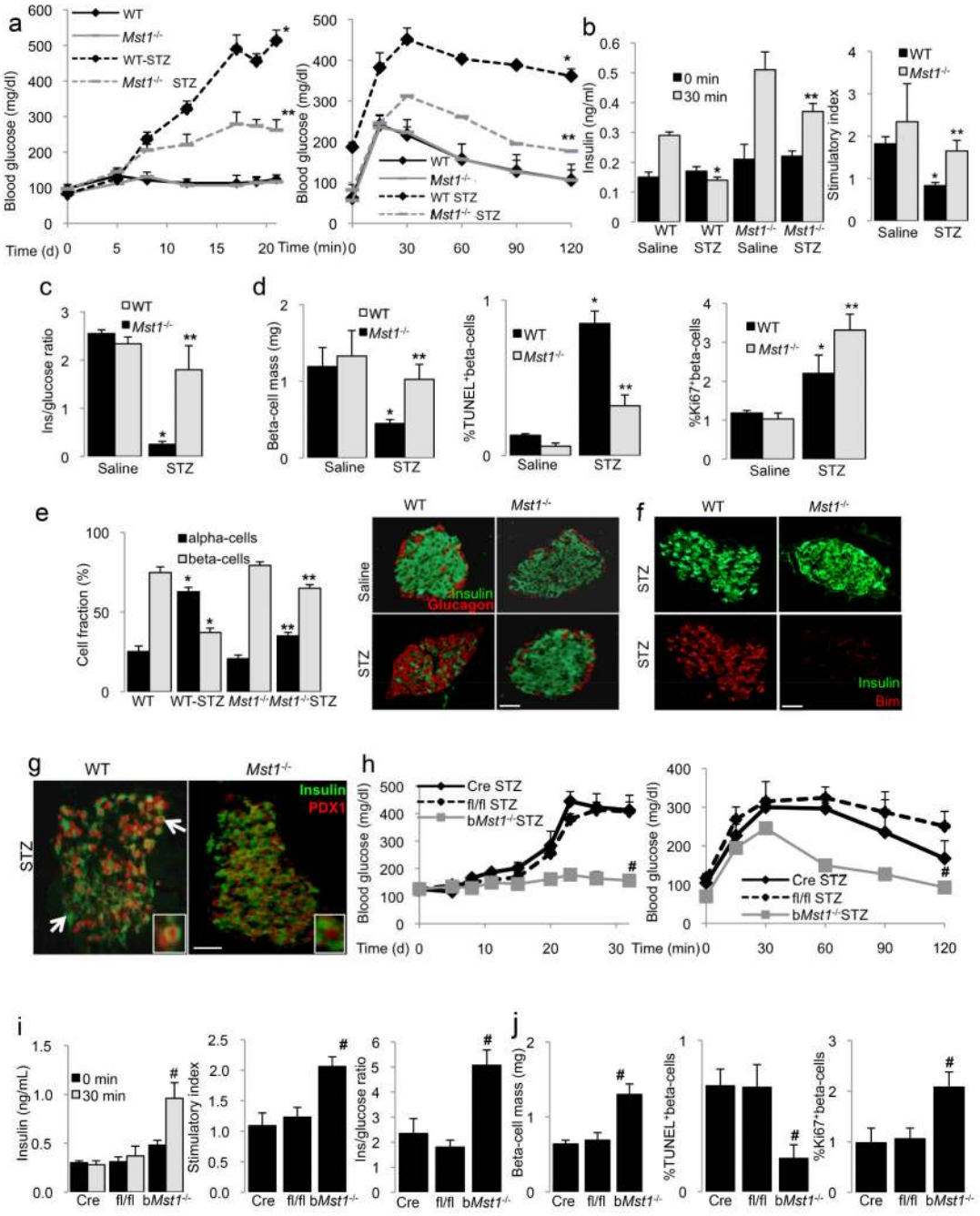

Figure 5. *Mst1* deletion protects from diabetes *in vivo*

(a-g) *Mst1*$^{-/-}$ mice (n=15) and their WT littermates (n=14) were injected with 40 mg/kg streptozotocin or citrate buffer for 5 consecutive days. **(a)** Random fed blood glucose measurements after last STZ injection (day 0) over 21 days and intraperitoneal glucose tolerance test (ipGTT) performed at day 17. **(b)** Insulin secretion during an ipGTT measured before (0 min) and 30 min after glucose injection and data are expressed as ratio of secreted insulin at 30 min/0 min (stimulatory index). **(c)** The ratio of secreted insulin and glucose is calculated at fed state. **(d-g)** Mice were sacrificed at day 22. **(d)** Beta-cell mass and quantitative analyses from triple stainings for TUNEL or Ki67, insulin and DAPI expressed

Europe PMC Funders Author Manuscripts

as percentage of TUNEL- or Ki67-positive beta-cells ±SE. The mean number of beta-cells scored was 23121 for each treatment condition. **(e)** The pancreatic area of alpha- (stained in red) and beta-cells (stained in green) are given as percentage of the whole pancreatic section from 10 sections spanning the width of the pancreas**. (f,g)** Representative double-staining for Bim (red, **f**) or Pdx1 (red, **g**) and insulin (green) is shown from STZ-treated *Mst1*$^{-/-}$ mice and controls. White arrows indicate areas of cytosolic Pdx1 localization and its total absence in WT-STZ mice. **(h-j)** b*Mst1*$^{-/-}$ mice with specific deletion in the beta-cells using the Cre-Lox system (n=5) and their Rip-Cre (n=3) and fl/fl controls (n=3) were injected with 40 mg/kg STZ for 5 consecutive days. **(h)** Random fed blood glucose measurements after last STZ injection (day 0) over 32 days and ipGTT at day 32. **(i)** Insulin secretion during an ipGTT measured before (0 min) and 30 min after glucose injection and data are expressed as ratio of secreted insulin at 30 min/0 min (stimulatory index). The ratio of secreted insulin and glucose is calculated at fed state (right panel). **(j)** Mice were sacrificed at day 32. Beta-cell mass analysis and results from triple stainings for TUNEL or Ki67, insulin and DAPI expressed as percentage of TUNEL- or Ki67-positive beta-cells ±SE. Data show means ± SE. *p<0.05 WT-STZ compared to WT saline injected mice, **p<0.05 *MST1*$^{-/-}$-STZ compared to WT-STZ mice. #p<0.05 b*MST*-STZ compared to fl/fl-STZ or Cre-STZ mice.

Europe PMC Funders Author Manuscripts

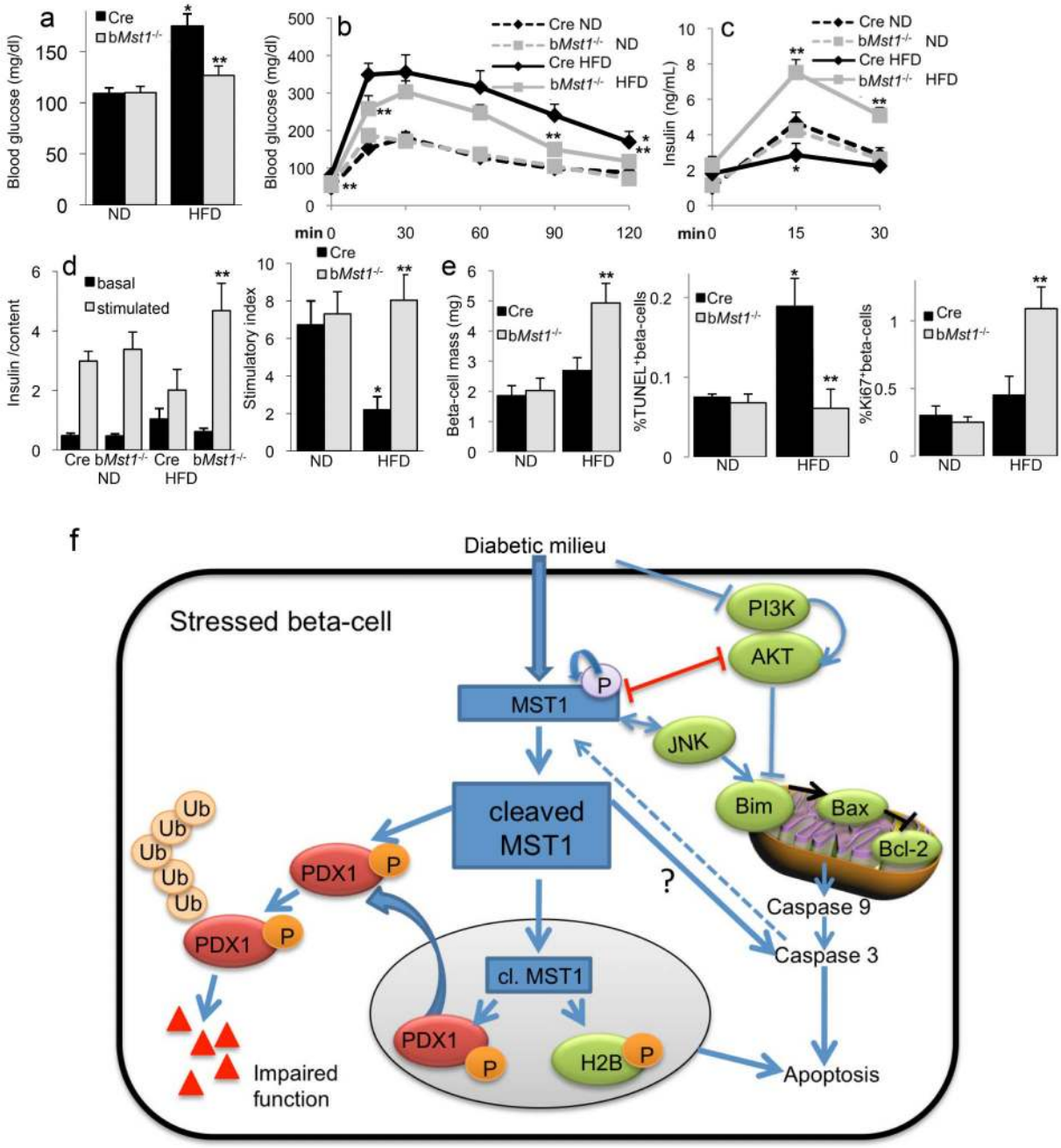

Figure 6. Beta-cell specific disruption of *Mst1* prevents hyperglycemia and high-fat diet induced diabetes progression

(a-e) *bMST1*$^{-/-}$ mice (fl/fl-Cre; n=12) and the Cre control mice (n=12) were fed a normal (ND) or high fat/ high sucrose diet ("Surwit"; HFD) for 20 weeks. **(a)** Random fed blood glucose measurements, **(b)** intraperitoneal glucose tolerance test (ipGTT) and **(c)** insulin secretion during an ipGTT measured before (0 min), 15 and 30 min after glucose injection. **(d,e)** Mice were sacrificed at week 21. **(d)** Islets were isolated from all 4 treatment groups, cultured overnight and subjected to an *in vitro* GSIS assay. Insulin secretion during 1h-incubation with 2.8 mM (basal) and 16.7 mM glucose (stimulated), normalized to insulin content. The insulin stimulatory index denotes the ratio of secreted insulin during 1h-

incubation with 16.7 mM and 2.8 mM glucose, respectively. **(e)** Beta-cell mass analysis and results from triple stainings for TUNEL or Ki67, insulin and DAPI expressed as percentage of TUNEL- or Ki67-positive beta-cells ±SE. The mean number of beta-cells scored was 23121 for each treatment condition. *p<0.05 Cre HFD compared Cre ND mice. **p<0.05 b*Mst1*$^{-/-}$-HFD compared to Cre HFD mice. **(f)** Our view on how diabetic stimuli lead to activation of MST1. Active MST1 triggers cytochrome *c* release and mitochondrial-dependent apoptosis by modulating Bim/Bax/Bcl2/Bcl-xL through JNK/AKT signaling. Active caspase-9 then triggers cleavage of caspase-3, which triggers the caspase-3-dependent cleavage of MST1 to its constitutively active fragment, which leads to further MST1 activation and processing of caspase-3 by a positive feedback mechanism, and acceleration of beta-cell death occurs. Cleaved MST1 translocates to the nucleus and directly phosphorylates PDX1 (we do not exclude the possibility that MST1 targets PDX1 also in cytoplasm) and histone H2B. PDX1 then shuttles to cytosol, where it marks for ubiquitination and subsequent degradation by proteasome machinery and beta-cell function is impaired. Histone H2B phosphorylation by MST1 also induces chromatin condensation, one of the characteristic features of apoptosis.